Hochschule Karlsruhe – Technik und Wirtschaft
Fakultät für Maschinenbau und Mechatronik

Deployable Thin Film Photovoltaic Array for Space Applications: Designs and Evaluation

*Bachelorarbeit (B.Eng.)

von

Felix Yves Bartsch

Hochschule Karlsruhe – Technik und Wirtschaft
Fakultät für Maschinenbau und Mechatronik

Deployable Thin Film Photovoltaic Array for Space Applications: Designs and Evaluation

*** V E R T R A U L I C H ***

*Bachelorarbeit (B.Eng.)
Nr. *B 18/059

von
Felix Yves Bartsch
geb. am 16.05.1993
in Karlsruhe
Matr.-Nr.: 48695

Betreuer des Deutschen Zentrums für Luft- und Raumfahrt (DLR)

M.Eng. Siebo Reershemius
Dr.-Ing. Patric Seefeldt
Dipl.-Ing. Torben Wippermann

Betreuer der Hochschule Karlsruhe (HsKA)

Prof. Dr.-Ing. Rüdiger Haas

Bremen, 03. 04. 2018 bis 03. 08. 2018

Satz und Herstellung:
Microsoft Office Professional Plus 2010
Microsoft Word – Version: 14.0.7194.5000 (32-Bit)
Font: Calibri, 11 pt
Druckdatum: 24. August 2018

Erklärung

Ich versichere hiermit wahrheitsgemäß, die Abschlussarbeit selbstständig angefertigt, alle benutzten Hilfsmittel vollständig und genau angegeben und alles einzeln kenntlich gemacht zu haben, was aus Arbeiten anderer unverändert oder mit Abänderungen entnommen wurde.

Karlsruhe, den 24. August 2018

Unterschrift:

S p e r r v e r m e r k

Diese Arbeit enthält vertrauliche Informationen. Veröffentlichungen bedürfen der schriftlichen Genehmigung des Deutschen Zentrums für Luft- und Raumfahrt.

Danksagung

Während meiner Zeit beim DLR habe ich viele neue Erfahrungen gesammelt, durch die ich mich fachlich wie auch persönlich weiter entwickeln konnte. Ich wurde im Team aufgenommen und meine Meinung wurde stets geschätzt. Dafür bin ich Allen, die mich im Laufe meiner Bachelorarbeit beim DLR begleitet haben, sehr dankbar. Besonderer Dank gilt meinen Betreuern, Siebo Reershemius, Patric Seefeldt und Torben Wippermann, die mich unentwegt unterstützt haben und mir immer mit Rat und Tat zur Seite standen. Auch Tom Spröwitz und Peter Spietz, welche immer ein offenes Ohr für mich hatten und mir jederzeit fachlich und organisatorisch zur Seite standen, möchte ich danken. Des Weiteren danke ich Thomas Renger und Maciej Sznajder, die mich wesentlich bei der Integration des Breadboard Models unterstützt haben.

Auf Seiten der Hochschule möchte ich meinem betreuenden Professor Rüdiger Haas danken. Er hat sich meines Themas angenommen und mir durch eine faire und unkomplizierte Betreuung den Rücken gestärkt.

Mit der Vollendung dieser Bachelorarbeit nimmt auch mein Studium ein Ende. In dieser herausfordernden Zeit erfuhr ich aus vielen Richtungen Unterstützung. Zum einen bedanke ich mich bei meinen Freunden und Kommilitonen für die gegenseitige Hilfe beim Lernen und dafür, dass sie mir mein Studium versüßt haben. Zum anderen möchte ich mich bei meiner Familie bedanken. Ich danke meinen Eltern und Großeltern, die stets an mich geglaubt haben und ohne deren finanzielle Unterstützung ich heute wohl nicht hier wäre. Annette Stegmann möchte ich danken, dass sie mich über die Dauer meines Studiums ohne zu zögern bei sich aufgenommen hat und mich immer mit allen Mitteln unterstützt hat. Abschließend gilt ein besonderer Dank meiner Freundin Sina Stegmann. Sie war immer für mich da und gab mir den Rückhalt und die Kraft mein Studium zu meistern.

Danke – Thank you!

Kurzfassung

Entfaltbares Dünnschicht Photovoltaik Array für Weltraumapplikationen: Designs und Evaluation

Ob kommerzielle Satelliten auf einer niedrigen Umlaufbahn der Erde oder Forschungssatelliten in den Tiefen des Weltraums, insgesamt zeichnet sich ein Trend zu immer höheren Energiebedarfe ab, der durch die herkömmliche Technik nicht mehr effektiv abgedeckt werden kann. Um eine höhere Energiedichte zu erreichen, setzt das Projekt GoSolAr (Gossamer Solar Arrays), des Deutschen Zentrums für Luft- und Raumfahrt (unter Führung des Instituts für Raumfahrtsysteme aus Bremen), auf die Verwendung von Dünnschicht Photovoltaik in Verbindung mit anderen dünnschichtigen Materialien. Daraus soll ein flexibles Solar Array entstehen, welches trotz einer geringen Masse und Stauvolumen die erforderliche Energie generieren kann.

Im Rahmen dieser Bachelorthesis werden hinsichtlich der mechanischen Umsetzung des Solar Arrays neue und durch den aktuellen Stand der Technik inspirierte Design Optionen erarbeitet und dem bestehenden Pool an Design Optionen hinzugefügt. Der Fokus liegt dabei in erster Linie auf der kritischen Phase der Entfaltung und der für den Transport notwendigen Verstauung des Solar Array Blankets. Die drei zu behandelten Design Parameter sind die Position, des für die elektrische Verbindung zuständigen Harness, dessen Faltung, und Strukturen, welche die Entfaltung unterstützen sollen. Da sich die unterschiedlichen Design Optionen teilweise auch parameterübergreifend beeinflussen, soll das beste Gesamtkonzept mithilfe einer technischen Evaluation bestimmt werden. Zusätzlich sollen Tests dazu dienen die Design Optionen besser zu verstehen um damit die Bewertung zu unterstützen.

Als wichtigster Design Parameter hat sich die Faltung des Harness herausgestellt, da diese den Entfaltungsvorgang maßgeblich bestimmt. Aus isolierten Entfaltungstests der einzelnen Design Optionen ging ein Faltungskonzept, welches ohne äußere Einwirkung im gefalteten Zustand verbleibt, als Vielversprechendstes hervor. Da sich dadurch das Blanket nicht von selbst und unkontrolliert entfaltet, kann beim Gesamtkonzept auf weitere Strukturen zur Unterstützung der Entfaltung verzichtet werden, wodurch die Komplexität signifikant reduziert wird. Abschließend wurde dieses Konzept, welches auch bei der Evaluation am besten abgeschnitten hat, als Breadboard Model umgesetzt und ersten einfachen Entfaltungstests unterzogen, wodurch die Entfaltung ohne zusätzliche unterstützende Strukturen als möglich bewiesen werden konnte.

Abstract

Deployable Thin Film Photovoltaic Array for Space Applications: Designs and Evaluation

Be it commercial satellites in a low earth orbit, or research satellites in deep space, overall, a trend towards higher energy requirements, that can no longer be effectively covered by conventional technology, is perceived. In order to achieve a higher energy density, the GoSolAr project (Gossamer Solar Arrays) of the German Aerospace Center (headed by the Institute of Space Systems in Bremen) relies on the use of thin film photovoltaics. In combination with other gossamer materials, a flexible solar array is obtained, which is able to generate the necessary energy despite its low mass and stowage volume.

Regarding the mechanical implementation of the solar array, new design options, inspired by the current state of the art, shall be developed and added to the existing pool of design options within this bachelor thesis. The focus primarily lies on the critical phase of deployment and the stowage of the solar array blanket, which is necessary for the transport to space. The three design parameters to be examined are the position of the, for the electrical connection responsible, harness, its folding, and structures to support the deployment. Since the different design options partially also influence each other across parameters, the best overall concept is to be determined with the help of a technical evaluation. Additionally, tests shall be done to gain a better understanding of the design options in order to support the evaluation.

The folding of the harness has proved to be the most important design parameter, as it has a decisive influence on the deployment process. Isolated deployment tests of the individual design options revealed a folding concept that remains in stowed configuration without external influence as the most promising. This prevents the blanket from getting deployed by itself and uncontrollably so that the overall concept does not require any further structures to support the deployment, by what its complexity gets reduced significantly. In a final step, this concept, which also performed best in the evaluation, was realized as a breadboard model and underwent first simple deployment tests, which proved that the deployment without additional supporting structures was possible.

List of Symbols

Ag	Silver
AHP	Analytic Hierarchy Process
BB-1	Breadboard-1
BB-2	Breadboard-2
CIGS	Copper Indium Gallium Selenide
CFRP	Carbon Fiber Reinforced Polyimide
CR	Consistency Ration
DLR	Deutsches Zentrum für Luft- und Raumfahrt (German Aerospace Center)
Flex PCB	Flexible Printed Circuit Board
GoSolAr	Gossamer Solar Arrays
GSA	Gossamer Solar Arrays
IKAROS	Interplanetary Kite-craft Accelerated by Radiation Of the Sun
InSight	Interior Exploration using Seismic Investigations, Geodesy and Heat Transport
ISS	International Space Station
JAXA	Japan Aerospace Exploration Agency
LEO	Low Earth Orbit
MLI	Multi-layer Insulation
NASA	National Aeronautics and Space Administration
PV	Photovoltaic
PVG	Photovoltaic Generator
SAW	Solar Array Wing
S/C	Spacecraft
SiO_2	Silicon dioxide

Contents

1 Introduction

Due to the progressing development of electrical spacecraft propulsion systems and the steadily growing demand for electrical power of today's S/C, "future commercial and deep-space satellites will require solar arrays with higher specific power densities than the current state-of-the-art, which is on the order of ~40 W/kg" ([1] p. 4). To achieve this, more efficient solutions are investigated to generate those high amounts of electrical power.

The GoSolAr project takes advantage of thin film photovoltaic technologies. In addition, other thin substrate and harness materials are used to gain a *Gossamer Solar Array* with a lower stowage volume and mass. The first goal is to develop and integrate a technology demonstrator with a span width of 5m x 5m for an in-orbit demonstration in LEO. This demonstrator shall provide the baseline for a scalable design of up to 20m x 20m.

1.1 Aims of the Work

As an entirely new technology the development of GoSolAr, especially the mechanical design and the electrical routing, need to be done almost from scratch. Therefore, new design options, regarding the mechanical aspects of the GoSolAr blanket, shall be acquired within this work and added to the so far existing ones. By the use of an evaluation, the accumulated design options shall then be investigated and contrasted with each other to gain the ideal GoSolAr blanket concept which is considered as the main outcome of this work. The evaluation shall also be supported by tests.

Additionally, this work can be seen as a listing of possible design options for the GoSolAr blanket. In case of future game-changing requirements, design options or else, beforehand rejected designs could then lead to an overall better concept and ergo should be estimated again.

1.2 Approach

The following work gets initiated with a state of the art review (Chapter 2). By reverse engineering space missions, projects, and their modules with similar aims as GoSolAr, the further design process shall be supported. Design options with respect to the mechanical

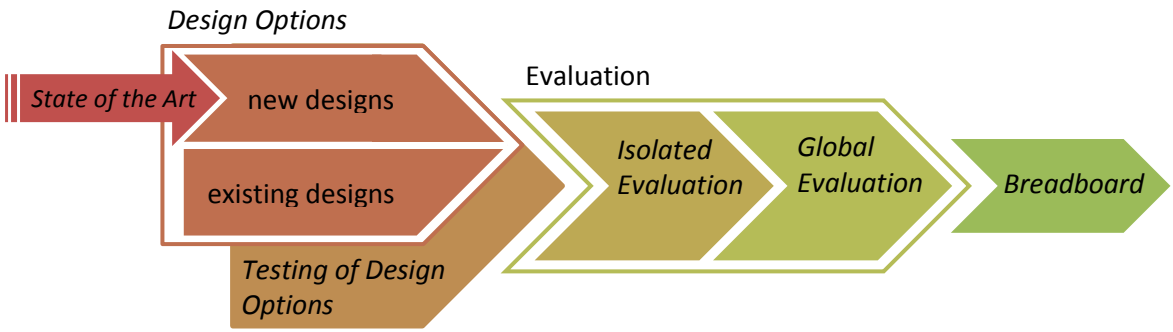

Figure 1.1 Illustration of the work's course of action

issues of the photovoltaic array, which are considered to have a greater potential, are then accumulated and described in Chapter 3. The design options refer to the position of the harness on the blanket, the 180° fanfold of the harness and possible deployment support structures. The testing of design options, shown in Chapter 4, shall provide further information about the design options and hence support the evaluation process. Primarily the deployment process of the design options was tested, making them more comparable with each other. The variety of design options and their reciprocal influence imply a greater difficulty of determining the best overall concept. To overcome this challenge, the evaluation is subdivided in two evaluation steps. Beginning with the so called isolated evaluation (Chapter 5), the design options shall be evaluated separately within their design parameter. This shall give a better understanding of the individual design options and also functions as input for the next evaluation step. With 13 different design options allocated to 3 design parameters the isolated evaluation shall be executed with a utility analysis. The global evaluation (Chapter 6) then defines possible overall concept, which guarantee a good interaction between the design options. Out of 3 concepts the best one shall be determined by the help of the analytic hierarchy process. Shown in Chapter 7, the best concept gets implemented as a breadboard model, which shall be used for future deployment tests. Chapters 8 and 9 are the final chapters containing the overall conclusion and outlook.

1.3 The GoSolAr Baseline Design

The GoSolAr blanket mainly consists of the thin film photovoltaic modules, a Flex PCB harness and an underlying membrane as a mechanical connection. The S/C itself is located in the center of the symmetric blanket. When stowed, the blanket (5 x 5 m²) is folded to a height of about 300 mm and in the XY plane to the size of the S/C (~500 x 500 mm²). The folding lines are turned 45° to the outer edges of the blanket and, except for the diagonal axis, are located between all neighboring photovoltaic modules and in both directions (see **Figure 1.2**). Thus, a two-dimensional folding pattern with fanfold is applied. Depending on the design options (Harness Position (A), Chapter 3.1) there are two 90° folds between the modules of either the Y or the X diagonal axis to accommodate the stowed blanket in a U-shaped configuration inside the S/C.

For the electrical connection, Flex PCB with a symmetric cross section and a total thickness of about 100 µm is used. Since the Harness gets folded in both directions when stowed, the symmetry of the Flex PCB is necessary to get the conductive copper in the neutral axis and therefore prevent series faults. There is no interconnection between generators on the blanket, and thus, several lines[1] from each generator to the S/C are unavoidable. Besides two harness types need to be distinguished. The column harness, one layer of Flex PCB, lies underneath one column of generators and leads to the diagonal axis where the separate main

[1] 2 power lines and up to 6 lines for sensors

harness is located. Other than the column harness, the main harness, which collects[2] the lines of the incoming column harness, leads to and inside the S/C and consists of several layers of Flex PCB.

The photovoltaic generators sit directly on the column harness, which they are also connected to. The cells are made of a Copper Indium Gallium Selenide (CIGS) semi-conductor. On account of this the total thickness of the cells can be kept to a minimum and a high power-to-mass ratio and volume efficiency can be aquired. In addition, the flexibility of the cells is another advantage for GoSolAr, although the photovoltaic generators (PVG) are not directly in the folded area. With the given size of 5 x 5 m² ($E_L \approx 5$ m) and PVG's of 20 x 20 cm² ($X_1 = Y_1 = 0.2$ m) a first approximate calculation of the maximum amount of PVG's on the blanket can be done:

$$\frac{1}{2} Y_3 + n \cdot Y_1 + (n-1)\, Y_2 + \left(X_1 + \frac{1}{2} X_3\right) \tan\alpha + \frac{E_W}{\cos\alpha} = \frac{Y_4}{2} = \sin \propto \cdot E_L \qquad (1.1)$$

$$n = (Y_1 + Y_2)^{-1} \cdot \left(-\frac{1}{2} Y_3 + Y_2 - \left(X_1 + \frac{1}{2} X_3\right) \tan\alpha - \frac{E_W}{\cos\alpha} + \sin \propto \cdot E_L\right) \qquad (1.2)$$

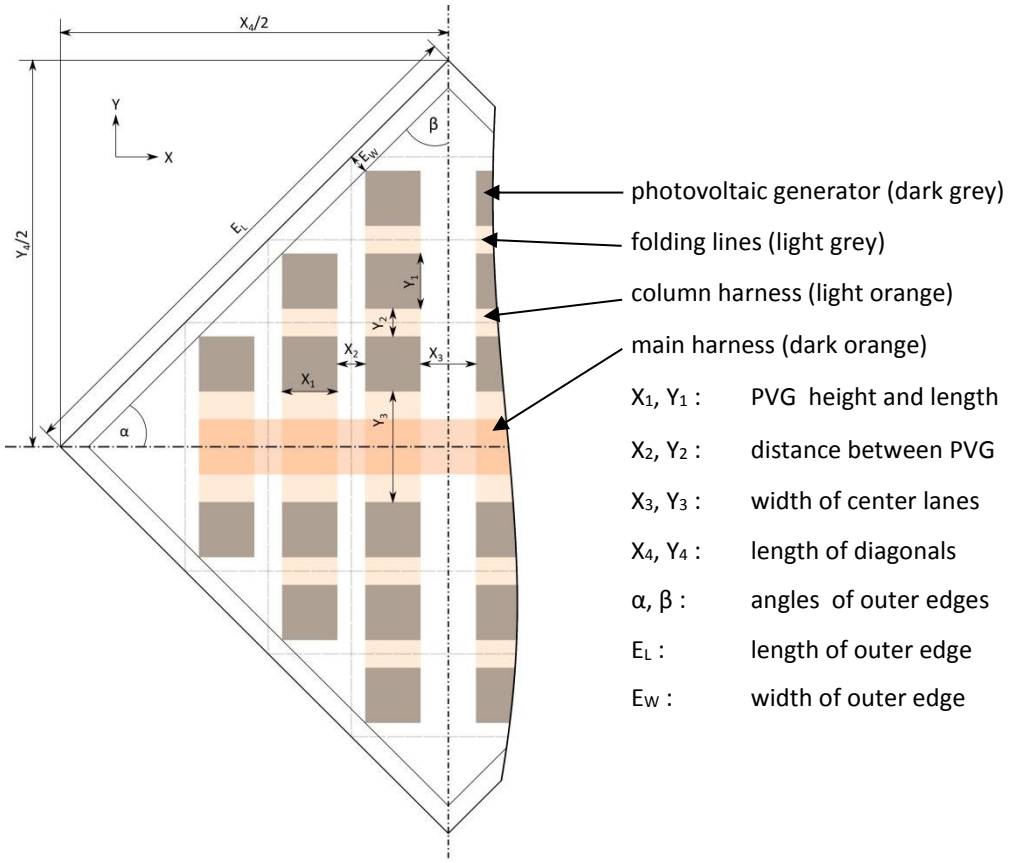

Figure 1.2 Basic layout of the GoSolAr Blanket (less PVG's) with all relevant dimensions

[2] Different design options have been developed but not further investigated so far and won't be part of this work.

With the assumption of a symmetric layout and all other, yet unknown dimension estimated ($X_2 = Y_2 = 2$ cm; $X_3 = 4$ cm; $Y_3 = 20$ cm; $E_W = 1$ cm) 15 PVG's on the diagonal axis on one quarter of the blanket (1.2), and therefore a total of 480 PVG's on the whole blanket can be arranged.

For deployment two deployment units are used to uncoil four light-weight, double omega booms (**Figure 1.3**) on the diagonal axis and from the center [2]. Each corner of the blanket is connected to the tip of one boom. At a time two booms, thus one axis of the blanket, get deployed completely. The booms, also referred to as collapsible tube masts, are made of Carbon Fiber Reinforced Polyimide (CFRP) [2]. For stowing, the booms are flattened and coiled up, to only take up a relatively small amount of space. Then, during uncoiling, the cross section of the booms[3] increases and therefore a stiff structure is provided [2].

Figure 1.3 Partially stowed double omega boom (DLR)

1.3.1 Materials

Apart from the thin film photovoltaic generators, polyimide foil is the primarily used material for the GoSolAr Blanket. The widely usage of polyimide in such a harsh environment as space, relates to its advantageous material properties. When travelling around earth, a S/C's materials need to withstand extreme temperature fluctuations. Polyimide accomplishes this due to its consistently good mechanical properties in a wide range of temperatures. Since the temperature of a material in space primarily depends on the materials reflexion, the polyimide (and other materials) can be additionally supported by Ag and SiO2 coatings to increase the reflexion and thus decrease its temperature when exposed to the sun. Another important property of polyimide is its low outgassing in vacuum. High outgassing products can condense on to the photovoltaic generators or in general on scientific instruments and thereby cause problems. Then again, polyimide has very good electrical insulation properties, which is why it is often used for electrotechnical applications. In the case of GSA, polyimide foil is not only used as a separate component (underlying membrane foil), but also in the form of Kapton tape and Flex PCB.

[3] The cross section in the direction of the deployment

Flex PCB stands for Flexible Printed Circuit Board. Those can be found in smartphones, computers, cameras and many other applications where flexibility is beneficial and only limited space is available. GoSolAr uses Flex PCB to electrically connect the generators with the S/C by simultaneously being able to fold the harness (Flex PCB). The Flex PCB consist of copper lines with a polyimide film as substrate layer, whereby the polyimide also ensures electrical insulation. Depending on the application, there can be either polyimide on one side or on both sides of the copper.

Kapton is the trade name for polyimide films developed by the American company DuPont. In combination with an adhesive layer it is commonly used as tape for space applications. As part of the GSA blanket, the Kapton tape ensures the mechanical connection between the blanket's components.

In general, adhesive methods are an advantageous joining procedure for the GSA blanket. Therefore, another suitable material for the mechanical connection is so called adhesive transfer tape, an adhesive layer without Kapton as substrate. The 3M adhesive transfer tape is also designed for high temperature exposure in combination with low outgassing properties.

The materials from above were also used for the breadboard models BB-1 (Chapter 4.1 p. 23) and BB-2 (Chapter 7 p. 45) and for the test harnesses of the harness folding tests (Chapter 4.2 p. 26).

2 State of the Art

To support the further design process, a state of the art research was done. It includes space missions, projects and their modules with similar aims as GoSolAr. The focus lies primarily on the mechanical aspects of the photovoltaic arrays in their folded and deployed state.

2.1 ISS

At present the International Space Station (ISS) is the largest single structure built by humans in space. Surrounding the Earth in an average LEO of 400 km it is used as a flying laboratory from so far 18 countries worldwide. [3]

Since the ISS wouldn't work without electrical power, it is equipped with 4 sets of solar arrays which can generate 84 to 120 kilowatts of electricity. The arrays, each with a wingspan of 73 meters, cover an area of about 2500 m². During transfer to space the solar arrays are folded like an accordion and deployed to its full-size once needed. The assembly of mechanical structure, harness, hinges and cells is further referred to as "blanket". [4]

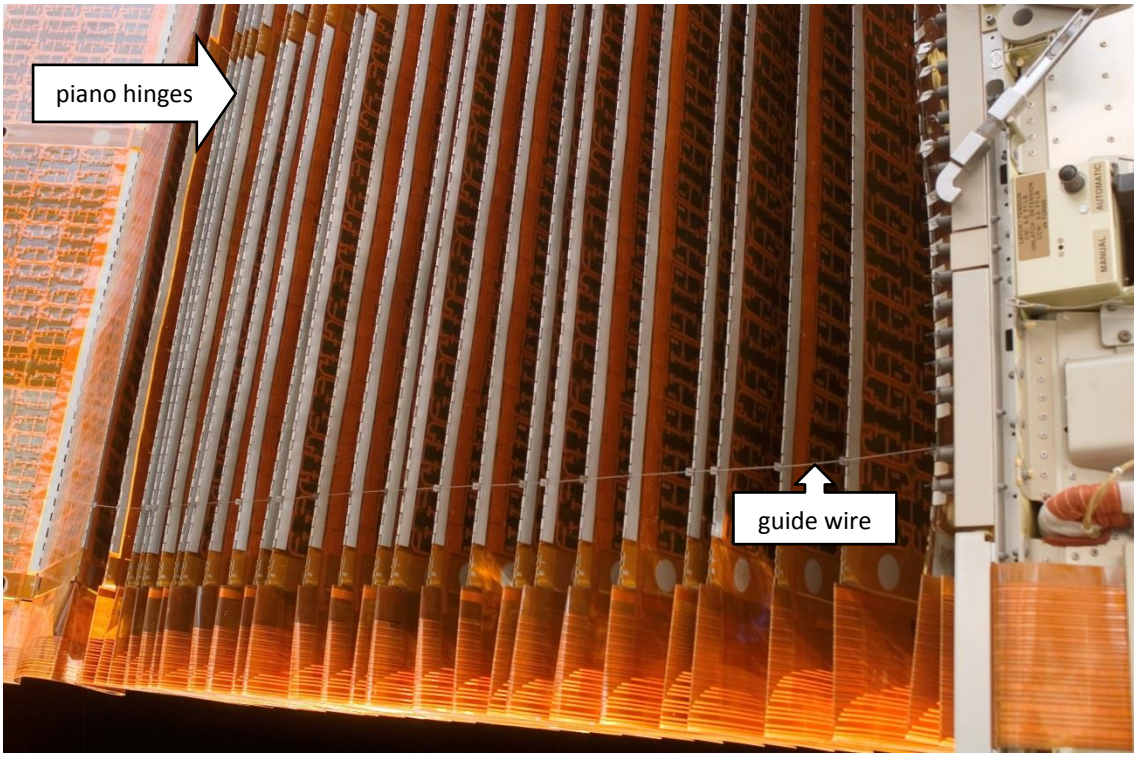

Figure 2.1 Close-up view of the port overhead Solar Array Wing on the International Space Station's P6 truss (NASA 2006)

To ensure this zigzag folding of the blanket, the individual photovoltaic modules are interconnected with piano hinges. The Flex PCB harness is routed on both sides parallel to the cells. The harness has some additional length at the piano hinges in order to assure proper bending radii. Violation of the bending radii can lead to ruptures in the electrical lines. Besides there is a guide wire implemented on the bottom side[4] of the array to support the deployment and folding of the blanket. The guide wire is threated through eyelets, which are connected to the piano hinges and therefore ensure a linear motion of the array, whilst deploying.

Due to the tight 180° turn of the harness, it is plastically deformed in this section, which can be seen even better when the blanket is deployed (**Figure 2.2**). Orthogonal to the piano hinges the modules are separated by metal bands. Those and the piano hinges accommodate the flux of force to deploy and flatten the blanket, so neither the sensitive PV nor the Harness have to sustain the main load. The holes in the metal bands are used to lock the blanket while folded. This is crucial so it is able to withstand the vibrations caused during launch.

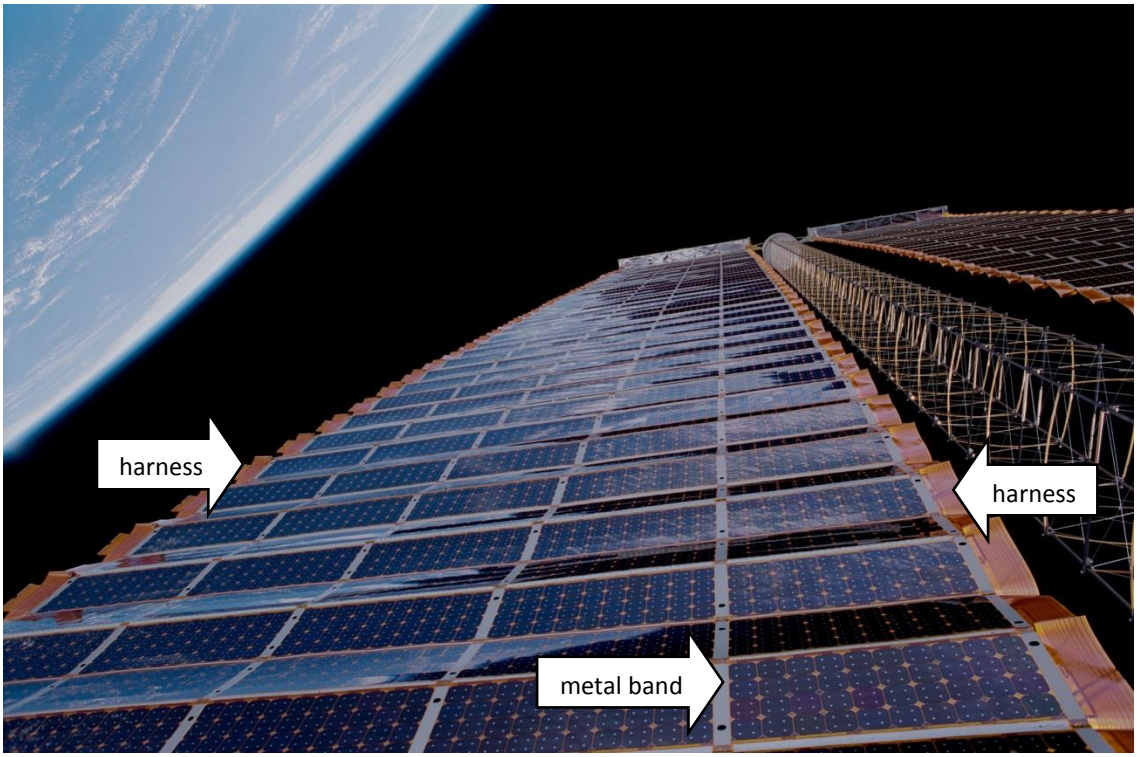

Figure 2.2 Deployed Photovoltaic (PV) Solar Array Wing (SAW) on the International Space Station‘s P6 truss (NASA 2000)

[4] Side of the array, which is not allocated to the sun

2.2 InSight Lander

The InSight (**In**terior Exploration using **S**eismic **I**nvestigations, **G**eodesy and **H**eat **T**ransport) lander is equipped with several instruments to study the deep interior of Mars. The main task of the lander is to first bring and deploy the instruments safely on to Mars' surface and then supply them with electrical power. [5]

Therefore, two UltraFlex[5] solar arrays are mounted to the lander. These have triangular shaped ultra-lightweight substrates (gores) which are connected together to a flexible-blanket. Thereby an accordion fanfold (**Figure 2.3**) can be accomplished to stow the solar array for transport. During deployment, each interconnected gore unfolds and becomes tensioned to form a shallow umbrella-shaped membrane structure, which, in fully deployed configuration, is inherently stiff and strong. This additionally is reinforced by the backbone formed by the stowage panels. [6]

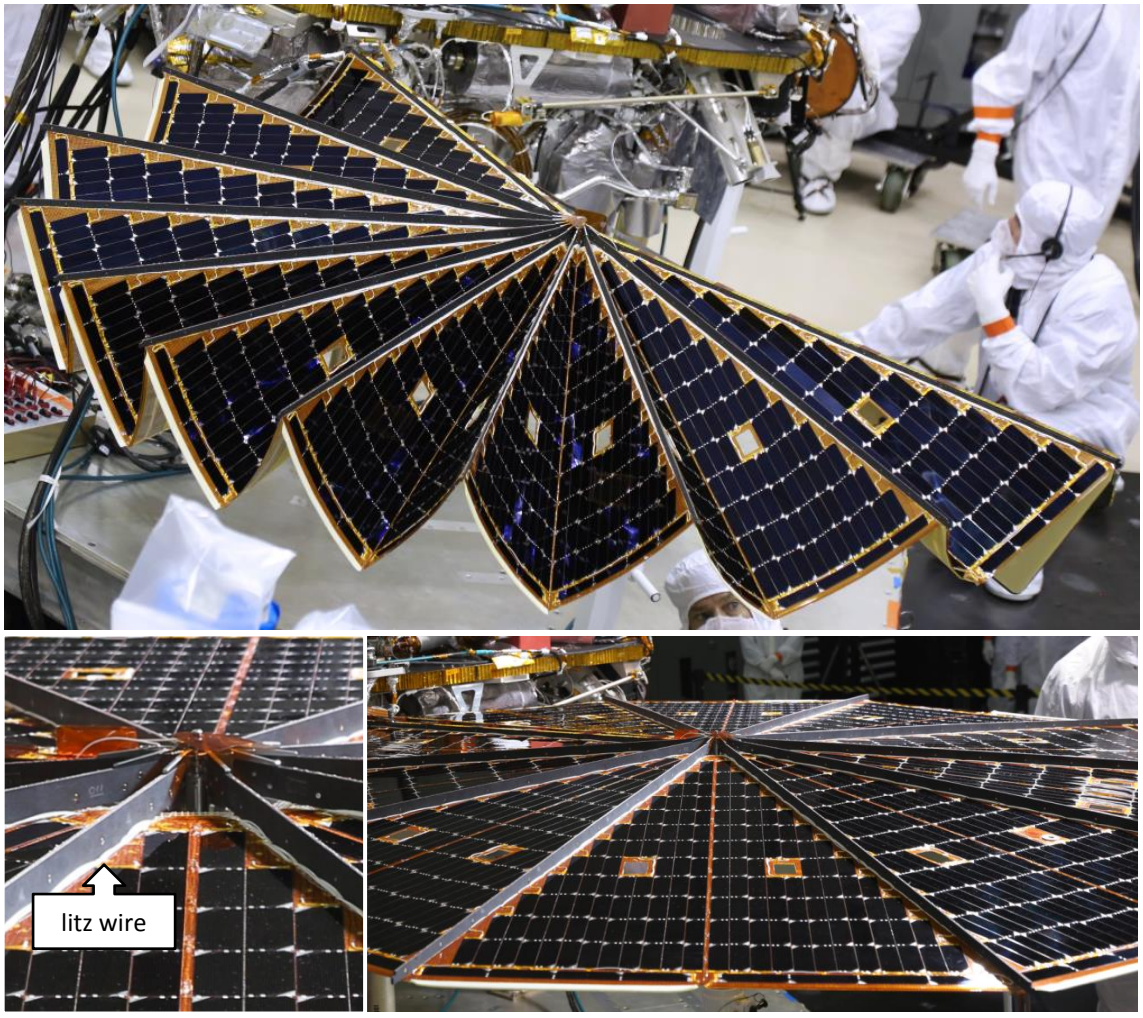

Figure 2.3 Top view of the deploying (top) and the deployed (bottom) Ultraflex solar array of the InSight Lander (NASA)

[5] UltraFlex is the trade name of the solar arrays, which are developed by Orbital ATK

The power generated by the solar modules is collected by common litz wires. They are placed on top of every fold (mountain and valley folds, but always on the mountain side) of the blanket and converge in the center of the solar array. Before they reach the actual S/C they are organized on the fixed stowage panel. Because the wires lie on top of the folds and also don't cross them, they just need to withstand a 90° turn at the fold but also a small amount of rotation in the center. Considering that, common wire with a circular cross section fits this application better than the often-used Flex PCB.

The wires are soldered to the PV modules and thus create an uneven blanket surface. To compensate this in stowed configuration, foam material is applied in a complementary zebra pattern to the bottom side of the blanket (**Figure 2.4**). However the stowed PV then still face each other and are in direct contact.

Rectangular holes in the middle of every gore are used to pass through a locking device to secure the blanket while stowed. One part of this device is mounted to each side of the stowage panels whereas the counterpart for both of them is on the middle gore (opposite side of stowage panel when deployed). It is not clear whether the blanket is only hold in place or also compressed.

The blanket's substrate seems to be made of polymide with an additional mesh structure to gain extra stiffness and strength. Though the whole blanket is not made of one coherent polymide substrate. The individual gores are attached to each other with either only the top or the bottom sides which makes the whole blanket more likely stay in stowed configuration because of the substrate's resilience .

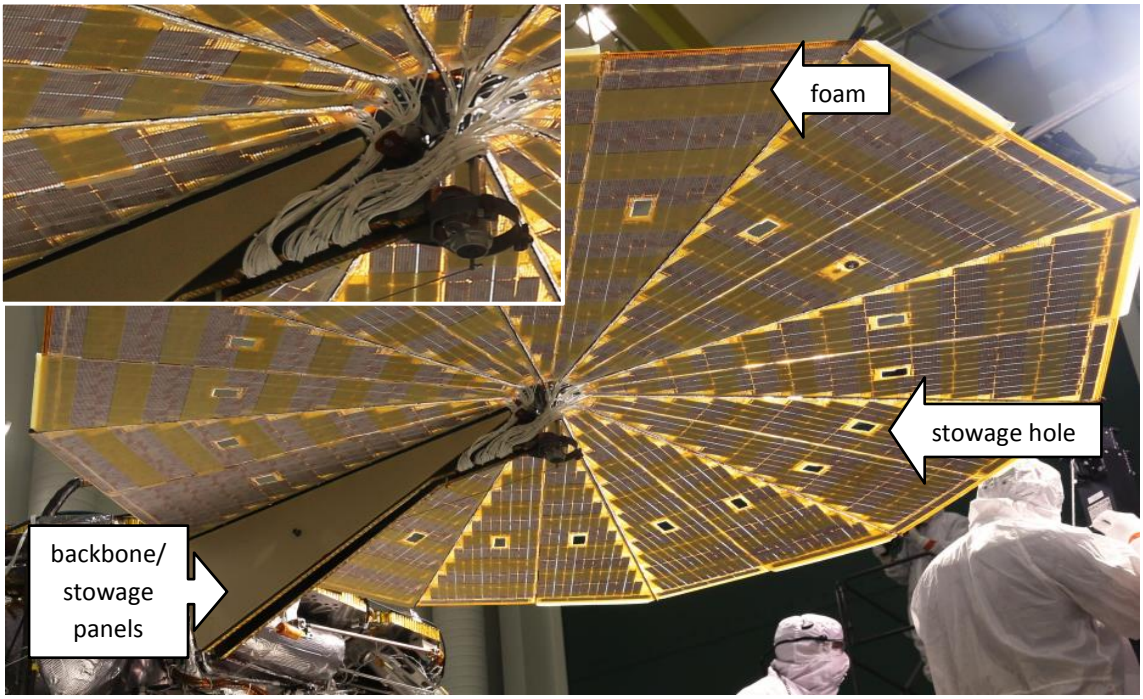

Figure 2.4 Bottom view of the deployed Ultraflex solar array of the InSight Lander (NASA)

2.3 IKAROS

IKAROS (**I**nterplanetary **K**ite-craft **A**ccelerated by **R**adiation **O**f the **S**un) was built by the Japan Aerospace Exploration Agency (JAXA) and is one of the world's first solar sailing demonstrators. Therefore, a large membrane converts the sunlight to propulsion force by using the impulse of the incident photons. Besides that, thin film solar modules are applied to the membrane to also demonstrate thin film power generation during its interplanetary cruise. [7]

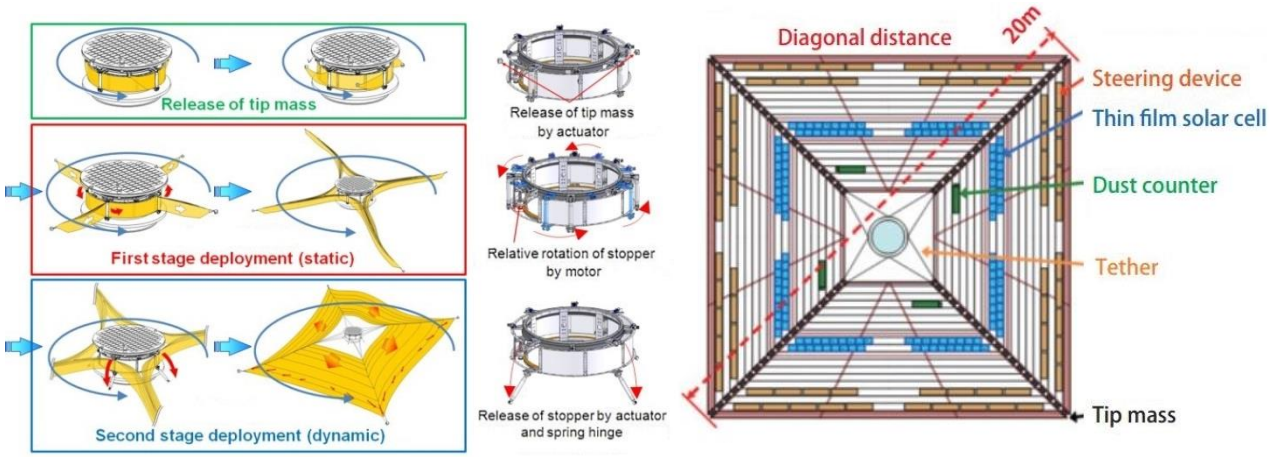

Figure 2.5 Left: Deployment of the IKAROS sail; right: sail shape and equipment layout (JAXA)

The sail is composed of four trapezoid petals, which together form a square with a diagonal distance of 20m. On each outer corner a tip mass is attached (**Figure 2.5**). This is needed to perform a spinning deployment, which consists of a static and a dynamic stage. In the first stage (static) the rolled petals are extracted and form a cross shape, maintained by the stoppers. Once the stoppers are released (dynamic stage), the sail drifts into its actual square shape. The centrifugal force is not only used to deploy the sail, but also to keep it flat. [7]

For electrical connection Flex PCB is located between the folds and on the diagonal axis of the sail. Since the sail is not only rolled, but also folded, the harness also needs to be folded (**Figure 2.6**). In this case the Flex PCB is plastically deformed in a 45° angle. In stowed configuration, there's also a fold approximately on the center lines of the square. Therefore, in this section no PV or other devices are applied, so they are only furled when stowed. (see Figure 2.5).

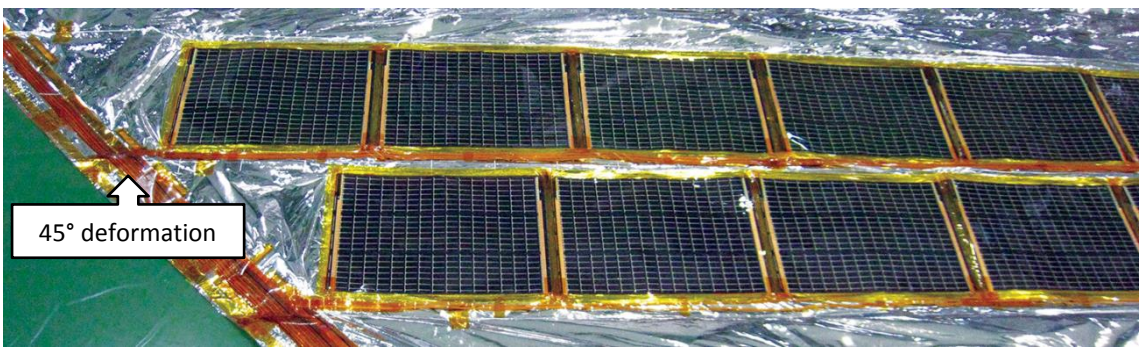

Figure 2.6 Thin film PV and harness routing on the IKAROS sail (JAXA)

3 Design Options

As for the mechanical issues of the photovoltaic array, several design options with greater potential have been accumulated. They refer to the position of the harness on the blanket (A), the 180° fanfold of the harness (B) and possible deployment support structures (E, D). Additionally, the current situation of the main harness design (C) is explained.

3.1 Harness Position (A)

In consideration of the volume of the stowed blanket, different design options for the harness folding have been developed. All three options have the same amount of PVG's on the blanket, but a slightly different blanket size, though the main difference lies within the folding of the blanket. Although the sequential[6] two-dimensional folding pattern with fanfold is given, the first and second deployment directions and the end of the fanfold are not yet determined.

3.1.1 Harness beneath Stowed Package (A-I)

In this case the diagonal axis with the main harness is folded in second place and therefore lies in the first deployment direction. After the blanket is folded in the first direction, the package of the zig-zag folded PVG's and the column harness are located on top of the main harness to gain a lower stowage volume compared to the other design options (**Figure 3.1**). When the second dimension of the folding is applied, the main harness alternately lies between and outside the PVG-stacks. This would only allow the use of a main harness with just a few layers to keep its thickness and therefore its bending radius at a minimum. Otherwise, with a thicker main harness, the gaps between the columns become too wide and the overall effectiveness of the blanket decreases. Another issue of this design is that the main harness, since it lies underneath the blanket when folded, is bound to the dimensions of the PVG's, especially if the homogeneity of the stowed blanket shall be assured. Additionally, and even more important, this quite big area cannot be used to accommodate PVG's.

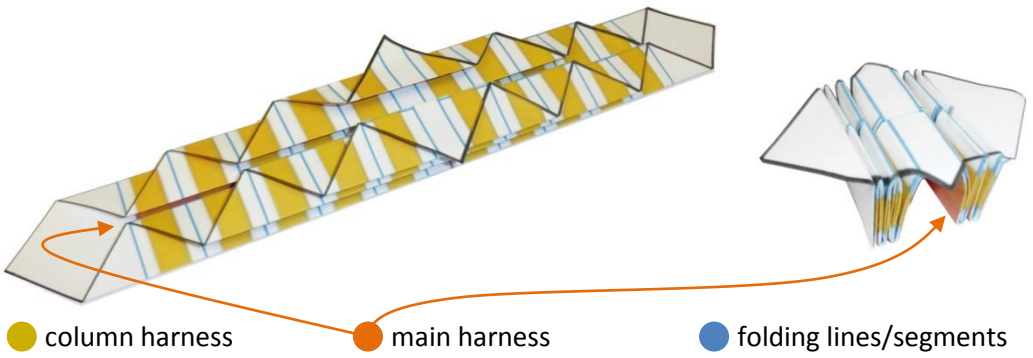

Figure 3.1 Paper model of design option A-I (Harness beneath stowed package), left: half folded/deployed blanket, right: stowed configuration

[6] One diagonal axis gets deployed completely before the other

3.1.2 Main Harness in First Deployment Direction (A-II)

As in design option A-I the main harness lies in the first deployment direction but without the PVG stack on top of it. The folding of the blanket in the first folding direction stops before including the main harness, which then lies separately in between the stacks (**Figure 3.2**). As a result, this design has the most impracticable stowing volume because of its stretched and longer shape. On the other side there are various advantages of separating the folding of the main and the column harness. Not only is the main harness independent in its design and dimensions, but also the overall design is getting less complex.

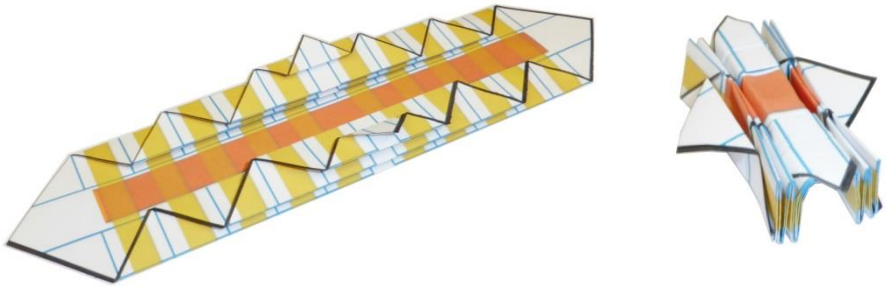

Figure 3.2 Paper model of design option A-II (main harness in first deployment direction), left: half folded/deployed blanket, right: stowed configuration, legend see Figure 3.1

3.1.3 Main Harness in Second Deployment Direction (A-III)

Similar to option A-II the main harness is arranged in its own row and not underneath the PVG stack as in A-I. The difference between design option A-II and A-III lies within the order of folding. For option A-III the column harness is folded first and the main harness afterwards (**Figure 3.3**). Therefore, a better stowing volume is combined with a separated main harness. However, the columns then lie on top of each other and up to 15 column harness layers need to get folded at once.

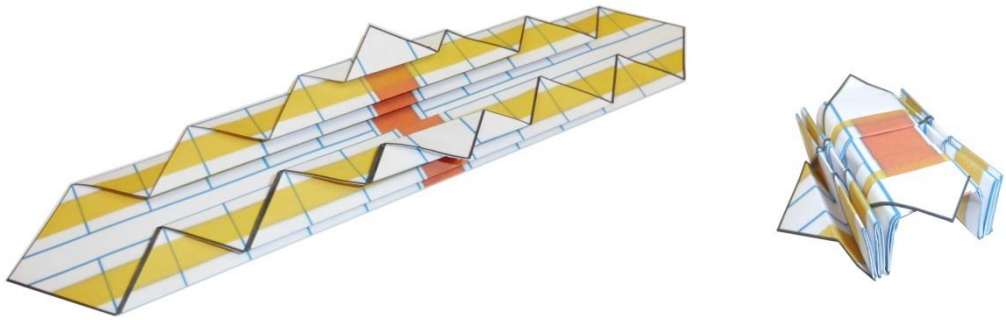

Figure 3.3 Paper model of design option A-II (main harness in first deployment direction), left: half folded/deployed blanket, right: stowed configuration, legend see Figure 3.1

3.2 Folding of the Column Harness (B)

The Flex PCB harness is the thickest and also stiffest to be folded material of the blanket. Because of this, the folding of the harness, particularly the column harness, is the most significant parameter of the whole design. Although the following options are primarily designed for the column harness they could also be considered for a main harness with only a few layers.

Regarding the elastic force of the deploying harness, in theory two extremes can be defined. Either the maximum elastic force is present in stowed configuration and decreases during deployment, or the elastic force of the harness appears during deployment and ascends to a maximum when deployed. The Position, the harness gets into by itself and without any external influences is referred to as *natural position* (**Figure 3.4**). If the harness generates high elastic forces when folded, it is necessary to use deployment support structures to prevent the blanket from unfolding by itself and thus deploying uncontrollably. On the other hand, a harness with high elastic forces at the end of deployment also means a higher or potentially a too high load on the booms.

Figure 3.4 Expected natural position of the harness options between stowed (left) and deployed (right) configuration (CAD models: DLR)

3.2.1 Elastic Deformation without Extra Length (B-I)

Option B-I can be considered as the extreme in stowed configuration. When deployed, the harness is in its original flat shape without any deformations, whereas when stowed, a high elastic force is generated due to the 180° bending (**Figure 3.5**). In order to realize an only elastically deformed harness, wider gaps between the generators are required. Due to the larger distance between generators less area of the blanket can be equipped with PVG and the overall effectiveness decreases. Even though this design implies a less difficult integration, an accurate stowing without any devices to lock the blanket in place, is almost impossible.

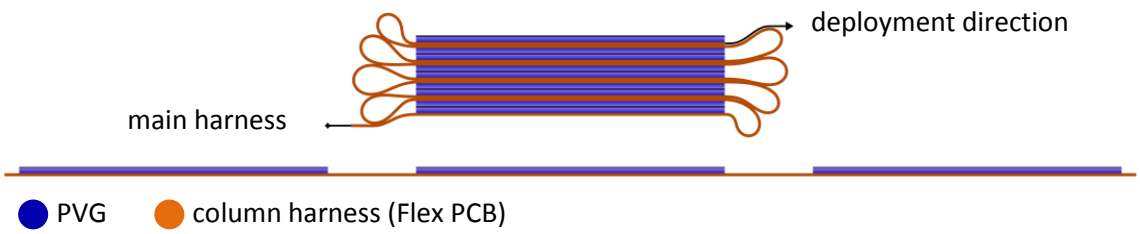

Figure 3.5 Sectional view of elastically deformed harness without extra length (B-I) in stowed (top) and deployed (bottom) configuration

3.2.2 Elastic Deformation with Extra Length (B-II)

To reduce the gaps between the PVG an extra length of the harness relatively to a subjacent membrane foil can be used. However, an extra length of the harness also makes the design and integration more complex, because the loop of the harness, caused by the extra length, alternately is situated on the front and back side of the deployed blanket (**Figure 3.6**). This design also has got the same stowing issue as B-I, although the natural position is considered to be somewhere in between stowed and deployed configuration (Figure 3.4).

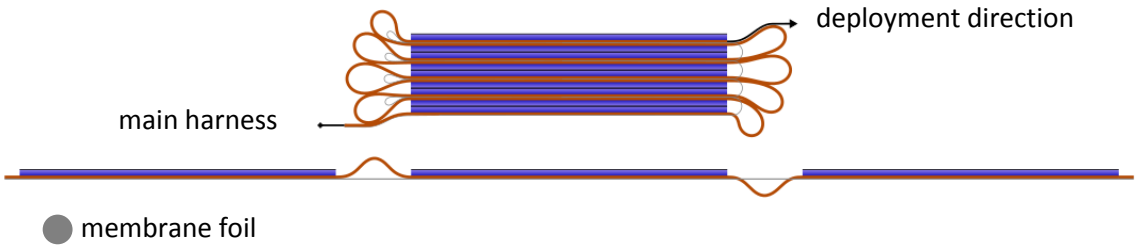

Figure 3.6 Sectional view of elastically deformed harness with extra length (B-II) in stowed (top) and deployed (bottom) configuration

3.2.3 Plastic Deformation (B-III)

With a similar natural position as option B-II, a plastically deformed harness can achieve even smaller gaps between the PVG's (**Figure 3.7**). At this concept, the harness is bend to its minimum bending radius. Any additional load from launch or integration can eventually reduce the radius, which might lead to damage in the electrical lines. Nevertheless, a plastically deformed harness can also be seen on the ISS solar arrays (Chapter 2.1) and on IKAROS (Chapter 2.3). In the case of a thin film blanket like GSA the plastic deformation of the harness not only leads to a smaller stowing volume, due to smaller harness loops, but also makes the blanket to lock itself in place when stowed.

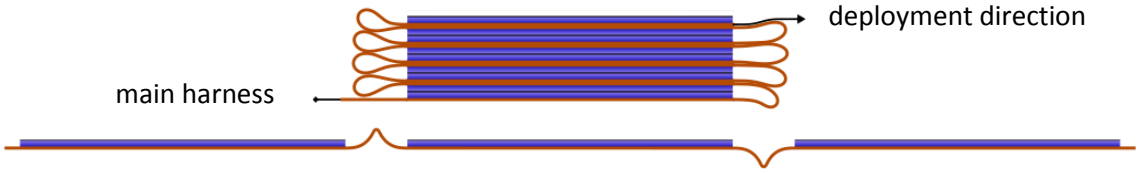

Figure 3.7 Sectional view of plastically deformed harness (B-III) in stowed (top) and deployed (bottom) configuration

3.2.4 Bottom to Bottom (B-IV)

The self-locking effect seen on option B-III exists even further for option B-IV. By attaching the harness to itself after the 180° turn (**Figure 3.8**), the natural position of this option shifts to stowed configuration. The loop of the harness can be realized with either an elastic or plastic deformation. Since the harness stays in stowed configuration and won't pop out by itself, deployment support structures might not be necessary for this option and the overall complexity of the blanket can be decreased drastically. On the other hand, it cannot be ensured yet, whether the booms can withstand the load to deploy a harness like this properly.

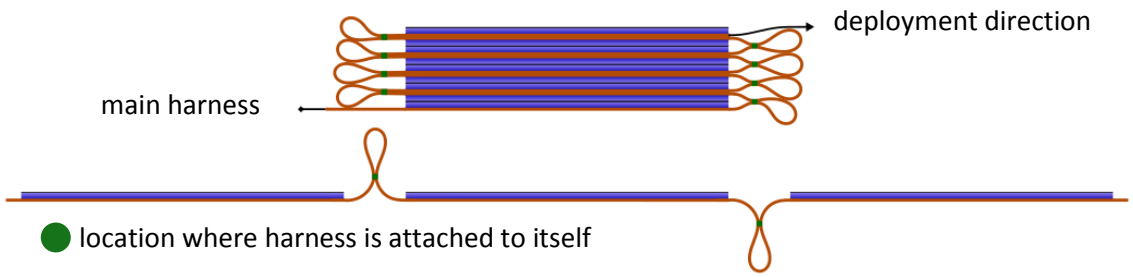

Figure 3.8 Sectional view of bottom to bottom harness (B-IV) in stowed (top) and deployed (bottom) configuration

3.3 Main Harness (C)

The design of the main harness is not yet determined, and shall not be further investigated in this work. Nevertheless, for the mechanical interaction between the different parts and hence the design options, it is necessary to know the layers of the main harness. For this reason, the current design situation of the main harness shall be roughly described.

The maximum possible amount of layers for one quarter of the blanket is the amount of column harnesses of one quarter. Thus, In the case of the technology demonstrator, 15 layers per quarter. However, the 15 layers would only occur at the close center and decrease by one layer each time the main harness passes another column harness. In this case, main and column harness consist of the same Flex PCB, because the column (then the main-) harness gets folded by 45° when reaching the diagonal axis. The 15 layers of each quarter can be piled to a stack of 30 harness layers (not possible for option A-I) to reduce the area, which is occupied by the main harness and therefore cannot be used effectively with PVG.

Another possibility is to use two separate Flex PCB's for the column and the main harness. Then the electrical connection between both needs to be ensured by soldering, adhesive bonding, connectors or else. In that case a minimum of one layer for the main harness could be sufficient.

The actual amount of layers most likely lies between both rather extreme options. One harness layer can't accommodate all tracks and therefore needs to be wider or preferably thicker than the column harness. On the other hand, a stack of 15 or even 30 layers of Flex PCB is barely neither foldable nor manageable. For option A-I nothing but a main harness with fewer layers would work out, since the main harness lies underneath the PVG stacks when folded.

3.4 Deployment Support Structures (D, E)

Regarding the life cycle of GSA, the deployment of its blanket is one of the most crucial phases. If necessary, so called deployment support structures shall be used to achieve a deployment, which to the greatest possible extent is predictable and controlled. They are subdivided in deployment support structures for the first (D) and the second (E) deployment direction.

3.4.1 Lamella Leaves in Stowage Box (D-I, E-I)

In stowed configuration, depending on the different folding options, the harness tends to generate a relative high elastic force. Thereby the blanket jumps out of the stowage box by itself, when released. To reduce this *pop out effect*, flexible lamella leaves are mounted to the stowage box, which prevent the blanket from popping out at once.

In the first deployment direction, the lamella leaves need to be perpendicular to the blanket and only on the opposite side of the deployed blanket's level (**Figure 3.9**). In second deployment direction, the leaves would be arranged parallel to blanket. In both directions, there is either only one lamella leaf at the front/top of the whole stack or furthermore lamella leaves in-between the column stacks. However, in second deployment direction the lamella leaves would only hold the four column-stacks in the center actively and the rest of the blanket only passively.

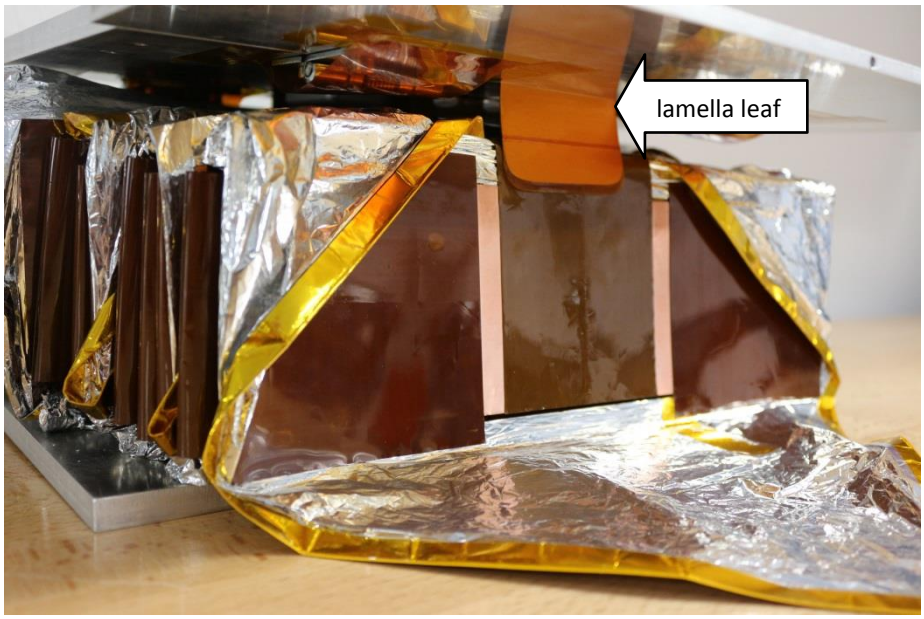

Figure 3.9 Breadboard model 1 in stowage box with a lamella leaf at the top to prevent the blanket from popping out

3.4.2 Guide Wires (D-II, E-II)

Guide wires, as seen on the ISS (Chapter 2.1), can also be suitable for the GSA blanket. A major advantage is, that a guide wire only allows linear motion in one direction. This is not only beneficial for the deployment, but also for stowing, due to the fact, that the blanket gets locked in place. Additionally, the overall stiffness of the blanket increases and could be increased even further if somehow the guide wire is not only connected to the booms' deploying end, but continuously to the booms. The guide wire system can be used on both deployment axes, though one boom axis has got a higher offset to the blanket than the other one due to the use of two deployment units.

In stowed configuration, similar to the booms, the guide wires sit on spools in the center of the S/C. The wires are threaded through eyelets on the blanket (Figure 3.10 left) and then connected to the boom-blanket interface. For deployment, the guide wires can be uncoiled by the same motors as for the booms, since both need to be deployed simultaneously. However, to achieve the same deployment speed, the different uncoiling radii due to the different material thicknesses needs to be considered therefore.

Figure 3.10 shows two concepts to accomplish a continuous connection between the guide wires and the booms. One possibility is to use loose loops on the booms which are able to move on the booms axis (Figure 3.10 middle). The loops are connected to the eyelets of the blanket, thus, the motion of the loops is only driven by the motion of the blanket. A better flux of force can be achieved with a loose spiral instead of loops (Figure 3.10 right). In this case the spiral gets deployed directly by the boom. Additionally, if connected to the opposite site of the blanket, the deployment force of the blanket can be compensated by the deployment force of the spiral and therefore the bending stress of the boom gets reduced.

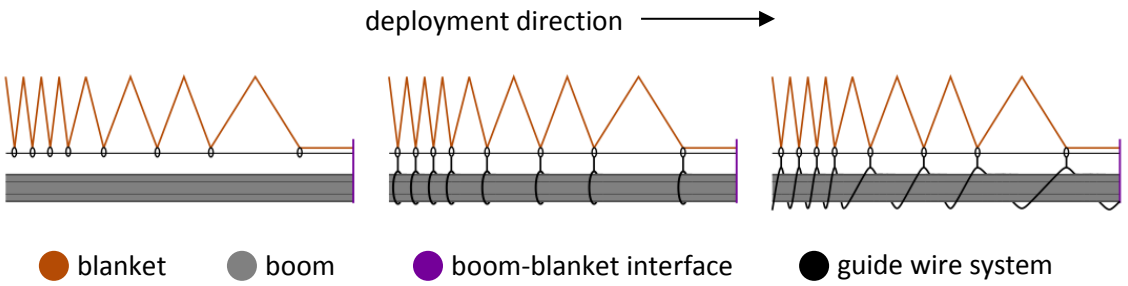

Figure 3.10 Guide wire systems during different states of deployment, left: no continuous connection between guidewire and boom, middle: continuous connection via loops, right: continuous connection via spiral

3.4.3 Friction Clips (E-IV)

In second deployment direction, the deployment can be further supported by friction clips. The clips hold the two halves of the blanket on every point, where the edges of the folded blanket face each other[7],together (**Figure 3.11**). Therefore, the clips are attached to one half, whereas the counterparts are attached to the other half of the blanket. Loops, attached to the undermost layer of the blanket, make sure, that the clips stay at the bottom and the blanket does not unfold itself. During the deployment of the second deployment direction, the clips get pulled open one after another, beginning with the ones close to the center, and thus release the intended part of blanket.

For other harness position options than A-I, friction clips are less effective. Due to the gap between the edges of the folded blanket, separate clips for both halves are necessary and a symmetric deployment can no longer be guaranteed.

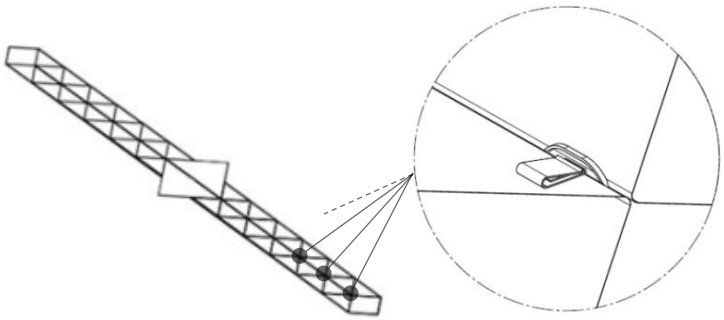

Figure 3.11 Position and detailed design of the friction clips on a blanket with an A-I design (DLR)

3.4.4 Lamella Leaves on the Blanket (E-V)

Intending the same goal as friction clips, lamella leaves represent an alternative solution for the harness position options A-II and A-III. This is because the flexible lamella leaves sit in the gap between the two folded halves of the blanket while also overlapping them to a certain point (**Figure 3.12**). During deployment, the rows of the fanfolded blanket get pulled out from underneath the lamella leaves one by one. In contrast to the friction clips, the lamella leaves have a better distribution of force but on the other side a symmetric deployment of both blanket halves cannot be assured.

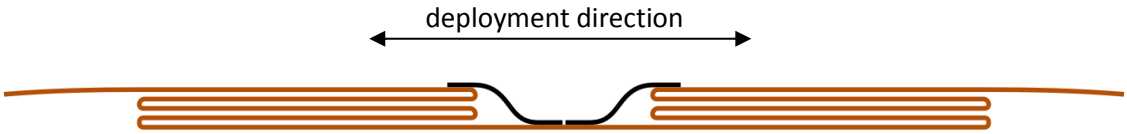

Figure 3.12 Simplified illustration of the lamella leaves on the blanket

[7] Only option A-I has got folded blanket stacks, which face each other directly

4 Testing of Design Options

4.1 Breadboard-1 Deployment Test

In the past, a first breadboard model (BB-1), including some of the stated design options, was built. The breadboard model is used for a first deployment test with actual models of the deployment units. This shall provide further information about the design options themselves, the interaction between them and the behavior of the overall concept.

4.1.1 Layout and Test Setup

The BB-1 (see **Figure 4.1**) has 7x7 PVG dummies on each quarter, ergo a total of 112. The PVG dummies sit on the column harness, which is attached to the main harness on the orthogonal diagonal axis. Every pair of column harnesses[8] has its own main harness. Therefore, the main harness layers increase by one after each column (A-II, C-max). The columns are connected via a membrane foil, which runs in-between the column harnesses from one edge of the blanket to the other edge. However, the membrane foil is not attached to the harness, but to the wider PVG dummies. Furthermore, the column harness is given an extra length relatively to the membrane foil. The elastically deformed harness with extra length (B-II) was almost impossible to handle without additional structures to keep it stowed, which is why the harness folding was changed to a plastic deformation (B-III). To be in control of the pop-out effect of the blanket, lamella leaves for the first deployment direction were installed in the stowage box (D-I). In the second deployment direction friction clips (E-V) are used.

The generator dummies have a layer stack of 50 µm adhesive on the bottom, 25 µm polyimide, 35 µm copper, 25 µm polyimide, 30 µm adhesive and 50 µm polyimide at the top. The column harness consists of a Flex PCB material with 50 µm polyimide and 35 µm copper, whereas the

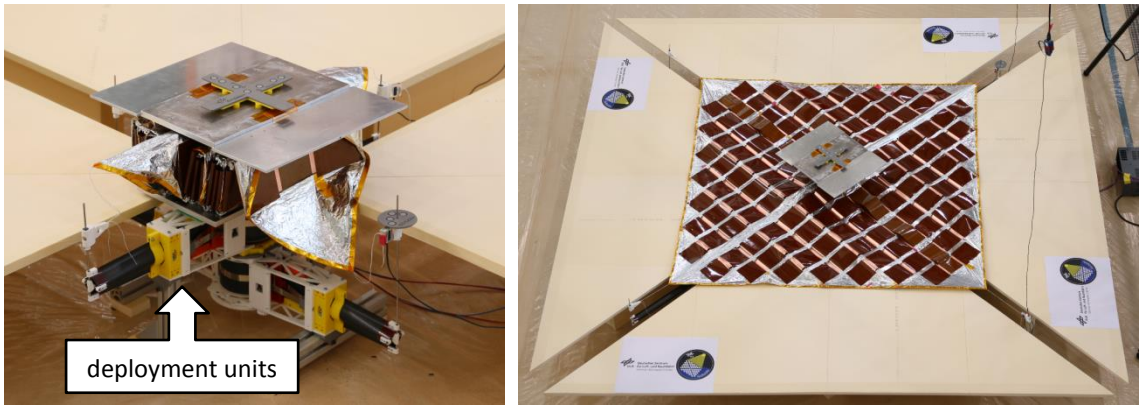

Figure 4.1 Setup of the deployment test of the breadboard model (BB-1). Left: stowed, right: deployed.

[8] A pair of column harnesses describes the two columns which are on the same line and face each other on the diagonal axis.

main harness is a symmetric Flex PCB with 25 µm polyimide, 35 µm copper and 25 µm polyimide (same material as for the PVG dummies). For the membrane, a 7 µm thick MLI foil is used.

The deployment tests were carryied out with models of the actual deployment units. As seen in Figure 4.1 the deployment units are positioned underneath the stowage box with the blanket inside. When deployed, the PVG dummies are facing upwards. The blanket gets pulled over plates, which are positioned on the deployed blanket's level, to reduce the effect of gravity. For the booms and the boom-blanket-interface, gaps are left between the plates on the diagonal axis of the blanket. Each axis is equipped with a force sensor, which is located between the boom-blanket-interface and the blanket. Additionally an optical position measurement is used

4.1.2 Results

The deployment tests revealed, that a blanket, which generates a higher elastic force due to the folding of the harness, is manageable by the help of deployment support structures, but furthermore also entails difficulties. In particular, a better understanding of the friction clips was gained through the tests. **Figure 4.2** shows the blanket during the deployment of the second deployment direction from top view. It can be seen, that the friction clips of the same deployment step do not open at the same time and thus cause an asymmetrical deployment, whereby a bending of the booms is induced. In addition, the jerky release of the blanket would cause the S/C to spin (in zero gravity). The irregular opening of the frictions clips can also be seen in the force-time diagram of the deployment (**Figure 4.3**). Depicted on the right side of the diagram, the course of the force sensor 2 shows a relative gentle increase, interrupted by two recurring peaks. Those peaks are caused by the friction clips, whereas the last peak constitutes the end of deployment. Additionally, it can be seen, that the loads, caused during the deployment of the second deployment direction, directly influence the load on the deployed booms of the first deployment direction. At the start, the influence is only little,

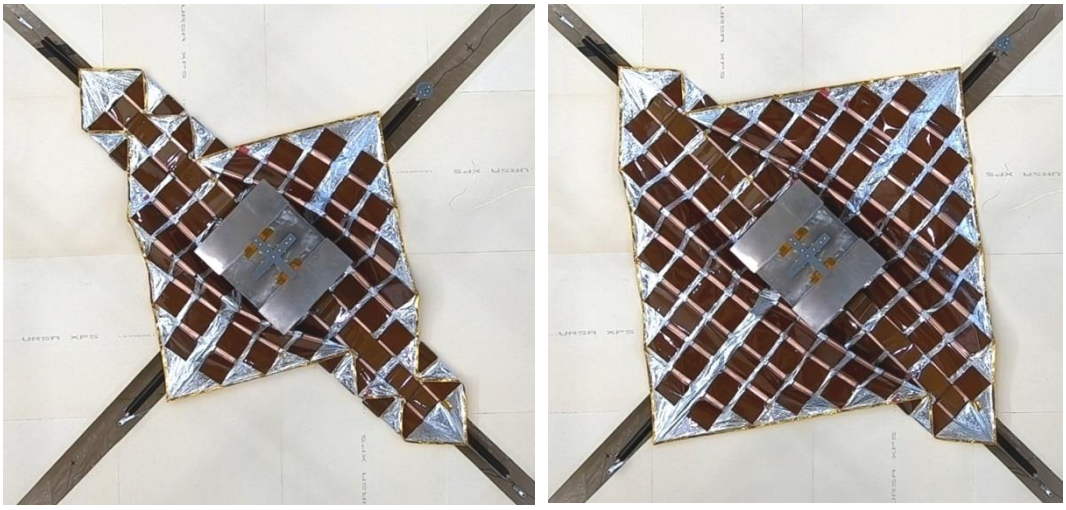

Figure 4.2 Top view of the blanket, during deployment in second deployment direction showing the irregular opening of the frictions clips.

whereas it increases during deployment. The reason for this is, that the tensile force on the friction clips, caused by the deploying booms of the second deployment direction, has a higher force component in first deployment direction, the further the friction clip is away from the axis of the second deployment direction. Not only the peaks of the friction clips get transferred to the booms of the first deployment direction, but also the increase at the end of deployment. In this case, the flux of force primarily runs through the outer edge, giving the whole blanket a higher tension.

The occurrence of peaks throughout the deployment of the first deployment direction (left side of Figure 4.3) can be attributed to the lamella leaves in the stowage box. Although, in contrast to the friction clips, the lamella leaves in the stowage box don't cause a bending of the booms, since those are on the boom's axis. Additionally, the peaks of the lamella leaves are way smaller than the ones of the friction clips, which are almost as high as the deployed state.

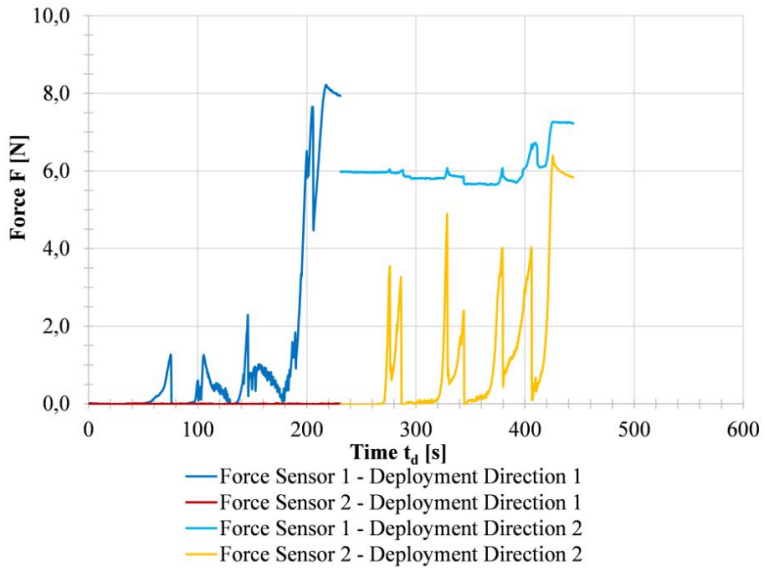

Figure 4.3 Deployment test run #2, force-time diagram, showing both deployment directions

4.2 Harness Folding Tests

Since the folding of the harness is a major design parameter, the evaluation shall be supported by tests to gain information's about the harness' behavior in stowed configuration, during deployment and when deployed, including the angles between generators and the progression of the force.

4.2.1 Test Setup

The test bench is shown in **Figure 4.4**. The key part is a linear guidance with a fixed bearing on the left side and a slide to simulate deployment on its right. The test object is located in the center of the setup. Via Kapton tape it is attached to even plates on both sides. The Kapton tape allows a rotary motion around the mounting point of the harness. This is necessary because for stowed configuration the harness needs to lay parallel in between the plates and when deployed it gets aligned perpendicular to the plates. In stowed configuration, the distance between the two plates is 5 mm. Because of burrs on the harness, caused by the hollow punch, the distance has to be bigger than the theoretical thickness of the layer stack of 2.1 mm. To reduce the effect of gravitation the test object is oriented perpendicular to the ground. Additionally, a low friction nylon cord, which is threaded through small holes in the top center of the test object, makes sure that the harness is in a straight line, without any curvature. On the right side, the nylon cord is clamped to the slide with a screw to allow a quick mounting and demounting of test objects. On the left side, it gets redirected and pulled down by a weight to maintain the tension. The nylon cord passes the left plate without touching it, so the only interaction among the cord and the test object, which influences the measurements, is the friction between them. However, the friction is neglected, since it is relatively small. For force measurement, a load cell is located between the fixed bearing and

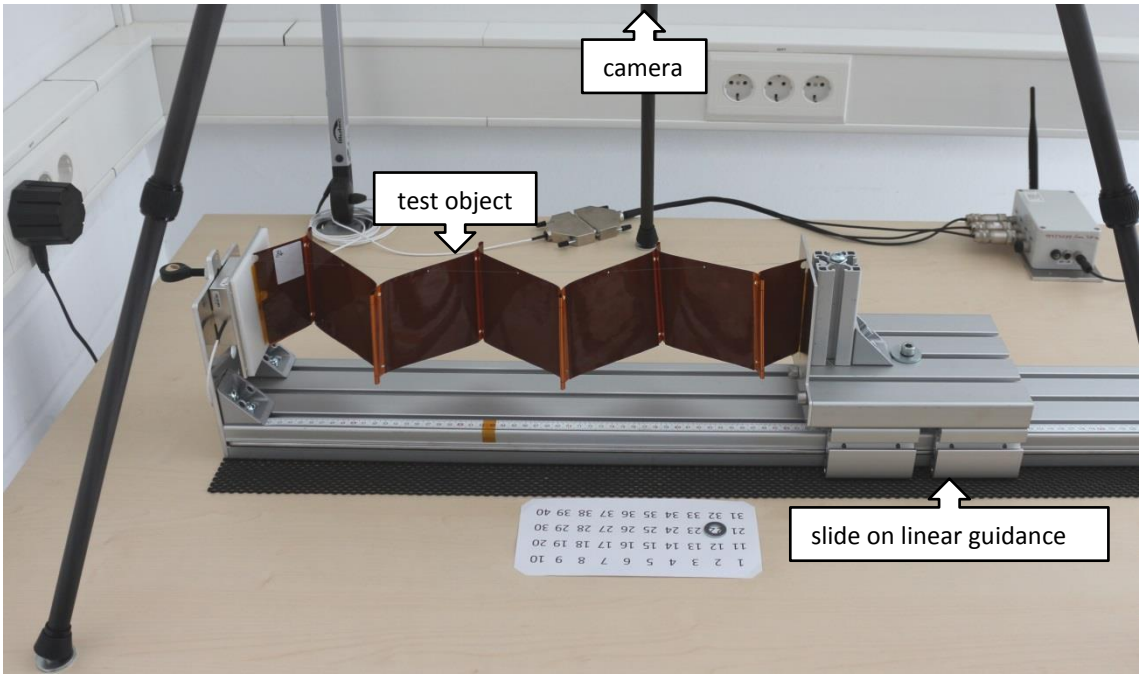

Figure 4.4 Overview of the harness folding test bench with harness folding option B-IV

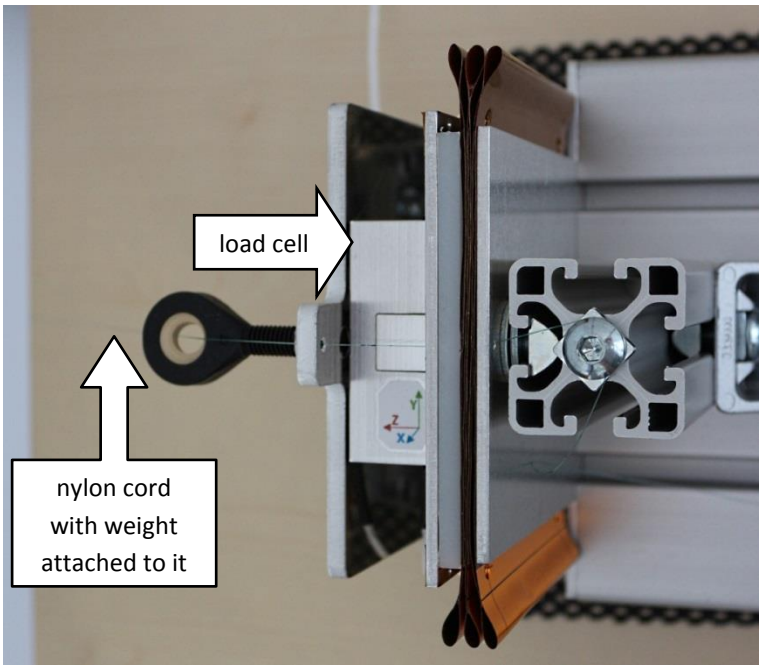

Figure 4.5 Close up view of the test bench in stowed configuration (option B-IV)

the plate on the left side, which holds the test object (**Figure 4.5**). The load cell is a 3-axis-force sensor K3D60 type from ME-Meßsysteme with nominal forces of Fx = Fy = Fz = 20N and an accuracy class of 0.5 %. Furthermore, a GSV-4BT M12 measuring amplifier with a 0.05 % accuracy from the same company is used. The test is carried out stepwise. For every measurement, the slide gets moved to the right by a few centimeters whereby the distance depends on the state of deployment. The crucial phases and therefore the phases with smaller steps, are at the beginning and the end of the deployment. The distance can be gathered from a scale underneath the slide. The slide can be fastened by a screw, which again is screwed to a slot nut, to prevent the slide from getting pushed or pulled away by the harness. With the help of a tripod, a camera is positioned above the test-bench. Throughout every step of the test a picture of the harness is taken by the camera. Afterwards, the pictures are analyzed to gain the relevant angles between the PVG.

The test objects themselves are made from Flex PCB with 5 whole and 2 half PVG dummies attached to them. Thus, there are 6 folds in total, 3 on each side. The Flex PCB has got a symmetric layer stack with 25 µm polyimide, 35µm copper, 25 µm polyimide. The PVG dummies are made of the same material but additionally with Kapton patches (50 µm polyimide + 30 µm adhesive) on the top and 50 µm adhesive on the bottom for the attachment to the harness. The whole harness column has got a width of 100 mm. The generators are quadratic with a side length of 100 mm, whereas the gap between the generators depends on the harness folding option. Besides the holes for the nylon cord there are 2 more holes next to each edge of the generators. In addition, with pins on the left plate, they were intended to lock the harness into position. It has however become clear, that this is not necessary due to the fact, that the locking effect of the nylon cord is sufficient enough.

Option B-I is realized with a gap of 25 mm between the generators. The gap between the generators of option B-II is 20 mm wide with a harness of 30 mm (10 mm extra length). For option B-III a gap of 15 mm was applied. Option B-IV has got a harness of 40 mm between the generators, which is sticked together at 7.5 mm with a 5 mm transfer tape (central axis of the tape). This results in a gap of approximately 10 mm when deployed. With the given gap widths, option B-I amounts to a total length of 750 mm, option B-II to 720 mm; option B-III to 690 mm and option B-IV to 660 mm in maximum deployed state.

4.2.2 Results and Comparison

The test results are shown in several diagrams, which support the further investigation of the properties of the harness folding options. The actual measured values can be found in the appendix (Table A.1 p. 61 - Table A.4 p. 64). With regard to the force, generated by the harness, the significant phases are the beginning and the ending of the deployment. The start is shown in a force-distance diagram (Figure 4.6), whereas the end is shown in a force-elongation diagram (Figure 4.7) to make the progression of force more comparable. Additionally, a force-angle diagram (Figure 4.8) shows the dependence of the force and the average angle between the generators.

Regarding **Figure 4.6**, the highest forces are measured right at the start of deployment. In this first section, the graphs decrease relatively quickly until about 1 cm of deploying. This first section describes the state of compression. In this state, the force, which is used to compress

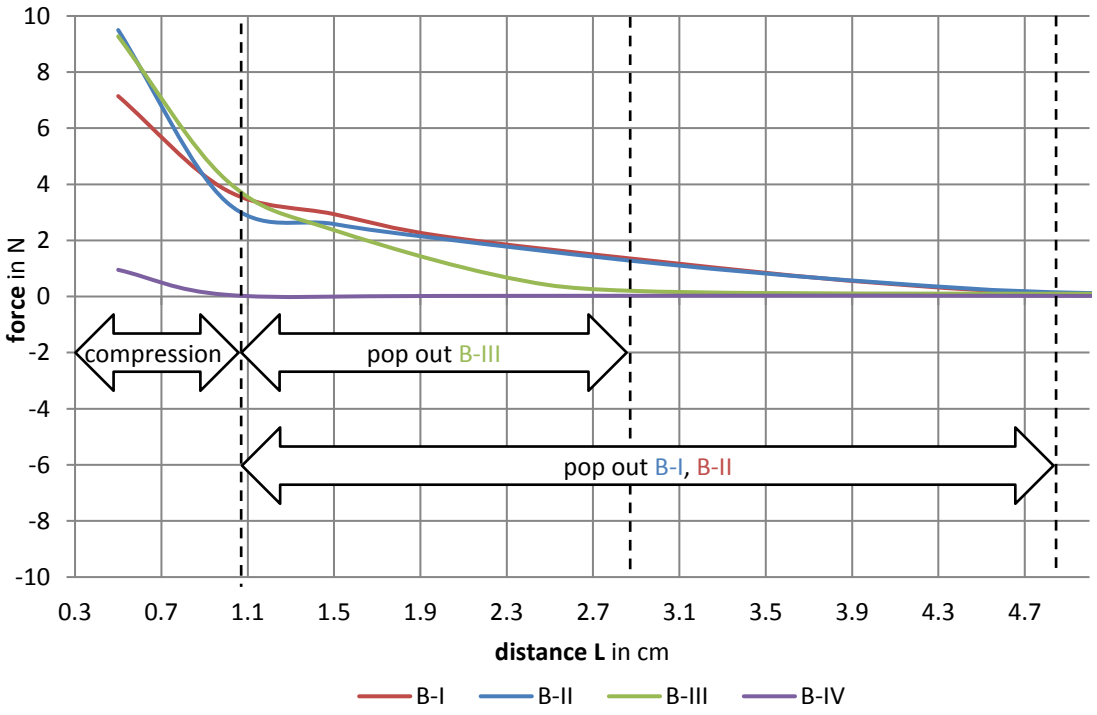

Figure 4.6 Force-distance diagram including all four harness folding options, zoomed in to the start of deployment.

the stack, is added to the force which is actually generated by the harness. After passing this point, the gradients of all graphs flatten, whereby option B-IV then already runs on the zero line. This confirms that the natural position of option B-IV is in stowed configuration. The other options leave the state of compression in the area between 2 and 4 N. However, option B-III falls to 0 N earlier than option B-I and B-II. The area between compression and 0 N gives an indication about the behavior of the harness, when released from stowed configuration without any deployment support structures. Due to the fact, that option B-III decreases faster a lower pop-out effect is assumed as for option B-I and B-II.

The graphs then stay at 0 N until approximately 80 % of deployment is reached. During the last 20 %, every graph has an individual course (**Figure 4.7**). Option B-I stays closest to the zero line and decreases suddenly right before 100 %. This is because option B-I only generates elastic force at the beginning but not at the end of deployment, since it then is in its normal, flat state. Option B-IV shows the opposite behavior. The graph decreases much earlier and smoother due to the elastic force generated throughout the final deployment phase. Option B-II and B-III behave similar to option B-I, though with a less sharp decrease. However, the quick rise of force at the end of deployment (B-I) also brings a higher risk of damaging the booms, because in this section, with every deployed mm, the force increases drastically. Ergo, with a smooth decrease, the deployed state can be figured out more reliable (B-IV). Another advantage of a smooth decrease and thus an early presence of elastic force is, that the blanket gets tensioned earlier. Thereby a bigger section can be considered for the deployed state for option B-IV as for the other three designs.

However, the actual deployed state is not yet determined. Contrasting the three deployment parameters (distance, force, angle), the angle between the PVG's is the most decisive parameter when it comes to sunlight received by the PVG and therefore the overall

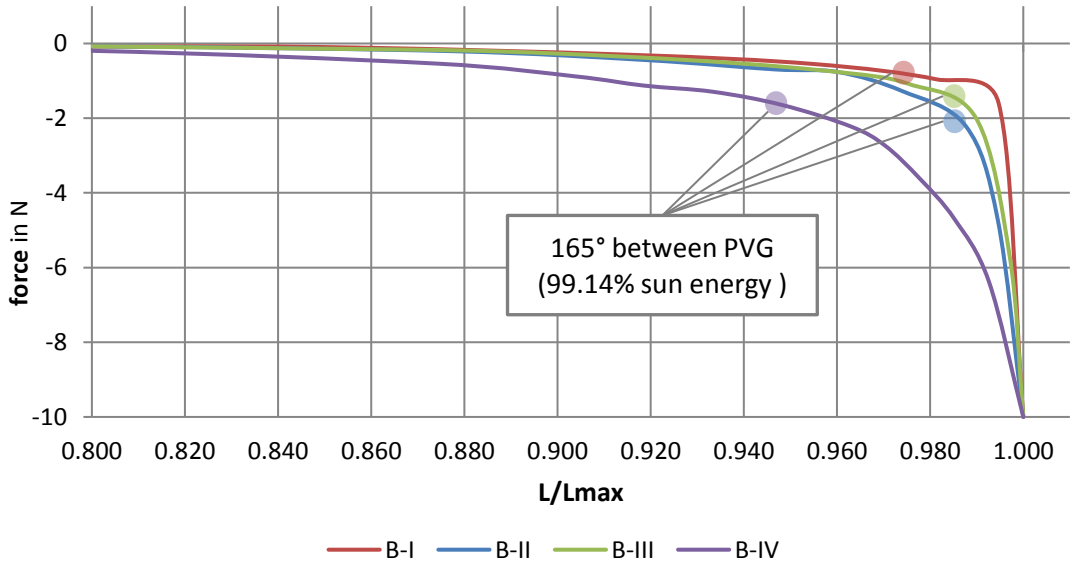

Figure 4.7 Force-elongation diagram including all four harness folding options, zoomed in to the end of deployment

effectiveness. Assuming the deployed state at an angle of 165° between the PVG, still 99.14 % of the sunlight's energy would reach the generators (calculation see p. 31). A remaining angle between the generators in deployed state can also be seen on the ISS solar arrays (Figure 2.2 p. 8). The position of the 165° angle is marked in Figure 4.7 (transferred from Figure 4.8). It can be seen, that, although B-IV needs a higher force to be deployed, it reaches deployed state earliest. Though, if the deployment force of option B-IV (or any other option) would be too high for the actual flight model, it still can be decreased by modifying the dimensions of the harness fold. Additionally, option B-IV (same with option B-II) has got a much lower spreading of the angles between the generators during the deployment (diagram, see appendix: Figure A.5 p. 65). For instance, at about 96% of deployment, the angles of option B-I spread from 137° to 162° (25° difference), whereas the angles of option B-IV lie in a range between 170° and 172° (2° difference). With a lower difference between the angles throughout the deployment and especially in the final phase, the deployed state can be determined better and the overall deployment is more predictable.

Figure 4.8 shows the force of the harness as a function of the average angle between the PVG. The top scale shows the sun energy which is received by the generators (calculation see p. 31). At 120° all 4 options almost need the same force for deployment. Afterwards they slowly start to move apart until about 160°, where every course changes individually. The sharp decrease (reverse scale of the force) of option B-I can be found again in this diagram. The other options decrease slightly smoother, whereas B-IV, again, decreases smoothest. Then again, with a deployed state at 165° (99.14 % of sun energy) the graphs of all four options show a similar course up to this point, although it needs to be taken into account, that Figure 4.8 depicts the average angles (spreading of angles is not considered).

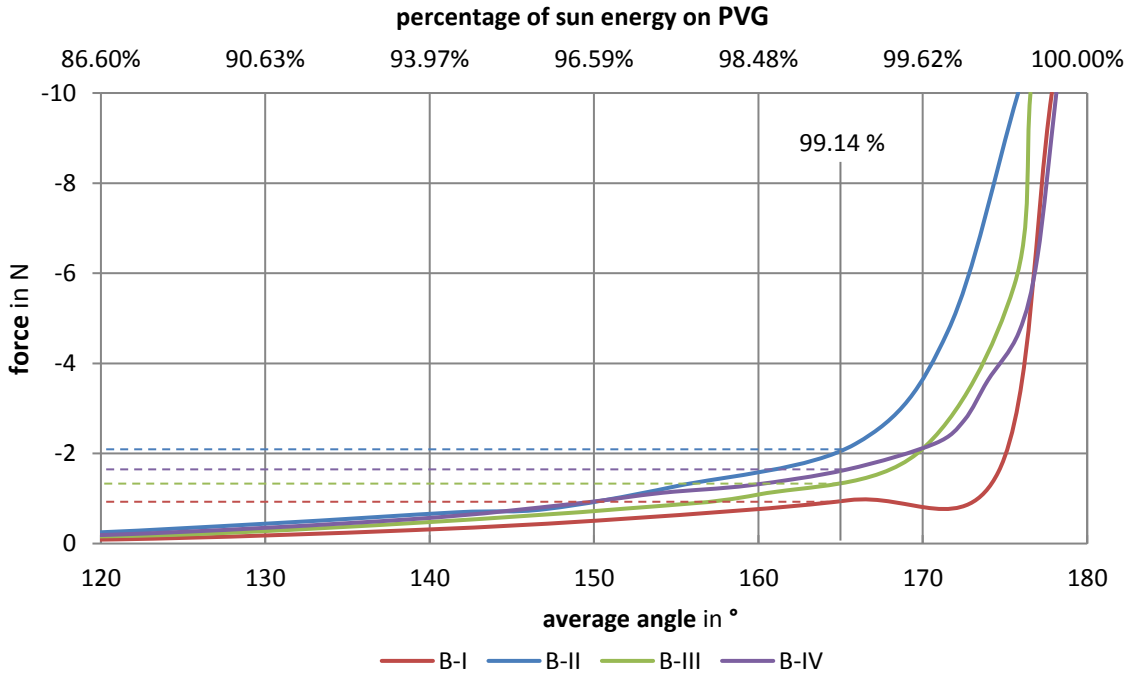

Figure 4.8 Force-angle diagram with the average measured angles of the four harness folding options, also showing the corresponding percentage of sunlight on the PVG

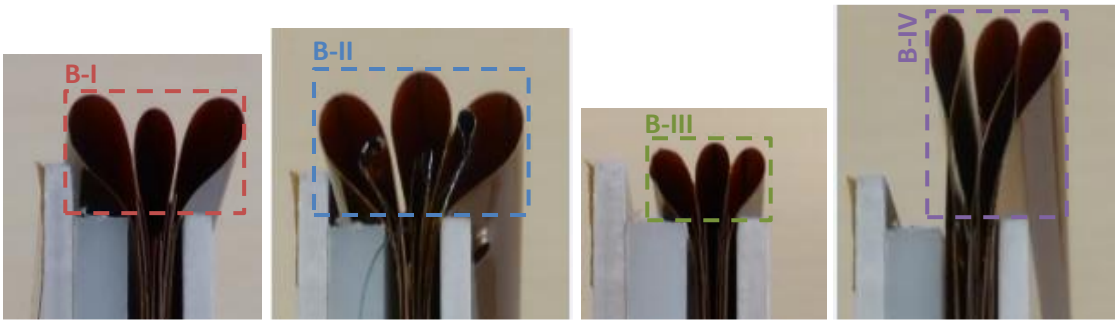

Figure 4.9 Harness loops in stowed configuration of all four harness folding options

Although the test columns were dimensioned only roughly, they can be used for a first comparison in terms of volume in stowed configuration. In **Figure 4.9** can be seen, that B-III needs the smallest stowing volume out of all four harness folding options, whereas the other three options take up a similar big space. However, the harness loops of option B.IV are longer and slimmer than the ones of B-I and B-II. This is a better condition, because the harness loops have a lower influence on each other and don't push one another away when stowed.

Calculation of the percentage of sun energy received by the PVG:

The vector of the sun energy (E_s) can be split up in in its individual components relating to the surface of the PVG (**Figure 4.10**). The relevant energy component is the one perpendicular to the PVG ($E_{s/PVG}$). With the perpendicular vector, the angle between $E_{s/PVG}$ and E_s (β) is the same as the angle between the PVG and the blankets plane and therefore can be calculated with the help of α (4.1). The wanted ratio of $E_{s/PVG}$ and E_s can then be expressed by the trigonometric relation between $E_{s/PVG}$ and E_s and β, whereby β can be expressed by α, which is the angle, measured in the tests (4.2).

$$\beta = \frac{180° - \alpha}{2} \tag{4.1}$$

$$\cos\beta = \frac{E_{S/PVG}}{E_S} = \cos\frac{180° - \alpha}{2} \tag{4.2}$$

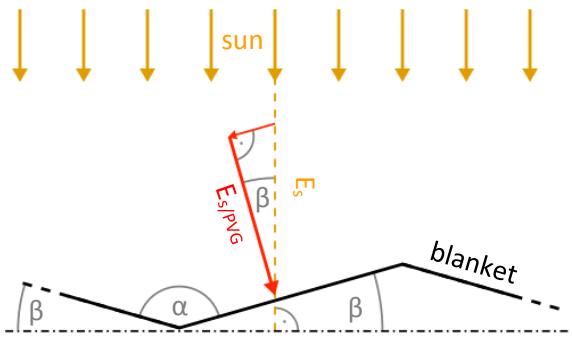

Figure 4.10 Illustration of the sunlight's energy received by the PVG/blanket

5 Isolated Evaluation

The accumulated design options shall be evaluated separately within their design parameter by the use of a utility analysis. With 13 different design options (A-I, A-II, A-III, B-I, B-II, B-III, B-IV, D-I, D-II, E-I, E-II, E-IV, E-V) allocated to 3 design parameters (A, B and D+E) a utility analysis is the better choice to gain reliable enough results with an appropriate work effort. Additionally, if new design options are developed in future, they simply can be added to the evaluation without doing the whole evaluation again. This also gets supported by the used naming (of the criteria and the design options) and the layout of the Excel sheets, which are used to perform the utility analysis. The results of the evaluation are also used to support the determination of possible overall concepts and therefore to support the next evaluation step.

The weighting factors for the utility analysis are determined by the use of a pairwise comparison (matrix) with a scale from 1 to 3 (**Table 5.1**). Thereby a rating of 1 means that the criteria compared to another one is less important, whereas a 3 represents that it is more important. A 2 stands for equal importance between both compared criteria. The weighting factors can then be red out of the matrix by normalizing the sum of the columns.

The actual utility analysis is done with the scale of the VDI 2225 guideline (Table 5.1). It spans from 0 to 4, whereas 0 stands for a disappointing, and 4 for the ideal performance of the particular design option. Every criterion of every design option is rated and multiplied by its weighting factor. The normalized sum then gives the total rating of the separate design options. Since the design options are only rough and not yet dimensioned concepts, the rating is done relatively to each and is also supported by the forerun tests. The matrices of the pairwise comparisons and the tables of the utility analysis can be found in the appendix (Table A.5 p. 67 - Table A.10 p. 72).

For the sake of clarity, the evaluation criteria, regardless of which evaluation step, are assigned to the four main phases of GoSolAr's life cycle, which are: *pre-launch activities, stowed configuration, deployment* and *deployed configuration.* If a criterion fits to more than one phase or to no phase at all, it is assigned to *general.*

Table 5.1 Scales for the isolated evaluation

weighting factors		
1	2	3
less important	equal	more important

utility analysis (VDI 2225)				
0	1	2	3	4
disappoit-ing	barely acceptable	sufficient	good	ideal

5.1 Harness Position (A)

5.1.1 Evaluation Criteria and Weighting (A)

Dimensioning, *integration* and *stowing* are assigned to the pre-launch activities phase. Although they belong to the less relevant criteria (see **Table 5.2**), they are taken into account by all three isolated evaluations. *Dimensioning* mainly regards the expected work effort needed and whether the dimensioning needs to be done from scratch or if similar technologies and methods are available. For the *Integration* criterion, the handling of the blanket, the amount of space needed and the complexity of the then to be done procedures are considered. Since the blanket will be integrated manually, another important aspect is the impact of failures on the whole blanket and whether damaged parts can be exchanged or in the contrary, how easy they can be damaged. When integrated, about 5 to 10 ground tests are planned for the actual flight model before it is send to space. This is one reason for the higher weighting factor of the *stowing* criteria. Additionally, a blanket which can be stowed better can also be handled better and therefore is considered as a good influence on the integration process as well.

In stowed configuration, the *volume* and *homogeneity* of the folded stack are of equal relevance. They are considered as the most important criteria for the harness position (A). The *volume* criterion gets described by the total size but also the outer shape of the stowed blanket. Subdivided in main and column harness, a high *homogeneity* is reached, when a blanket stack mostly consists of the same material without air pockets and the layers precisely lay on top of each other. In the case of the harness position, the accuracy of the stacks is regarded primarily, because if the edges of the PVG's lay on top of each other precisely, the stack is consistently homogeneous and can be compressed better.

The ratio between the blanket area and the area accommodated by PVG's shall be addressed by the criterion *PVG area*. Since the *PVG area* has got a high influence on the overall effectiveness of the blanket it also has got a high weighting factor.

Table 5.2 Evaluation criteria and weighting factors of design parameter A (harness position)

pre-launch activities			*stowed configuration*		*deployed*
A 2.1	A 2.2	A 2.3	A 3.1	A 3.2	A 5.1
dimensioning	integration	stowing	volume	homogeneity	PVG area
8.33	13.33	15.00	21.67	21.67	20.00

A 3.2.1	A 3.2.2
main harness	column harness
40	60

5.1.2 Evaluation of the Harness Position Options (A)

Compared to option A-I and A-III, option A-II doesn't influence the *dimensioning* of the blanket and therefore has got the highest rating of 4 points. Option A-I only gets 2 points because the main harness underneath the blanket stack increases the complexity of the whole design. The reason of the low rating of 1 point for option A-III is the stack of column harnesses, which needs to get folded at once. Due to the same reasons, as for the *dimensioning*, the *integration* of the three options is rated. The loops of the main harness of option A-I, which need to fit through the gaps between the columns not only make *dimensioning* and *integration*, but also the *stowing* (2 points) more difficult. The *stowing* of option A-III is also considered sufficient, due to the column harness stacks, and therefore gets 2 points as well. With a clean fanfold for the column harnesses and a separated main harness, option A-II gets 4 points for its *stowing* properties.

In terms of *volume,* option A-I ranks best with 4 points, because it takes up the smallest space and has got the most quadratic shape, which makes it fit best on the satellite. The *volume* distribution of option A-II is not ideal and in addition with its long shape only 2 points can be given. Option A-III is seen as a compromise of both, option A-I and A-II, and therefore gets 3 points. For the rating of the *homogeneity*, the *main* and column *harness* are regarded separately. With a two-dimensional folding pattern, the first folding direction is a fanfold with one layer and consequently the second folding direction has to be done with an increasing number of layers. A one layered fanfold is considered to gain a greater accuracy which leads to a better *homogeneity* over the whole area between folds. Options A-I and A-II have a main harness with an increasing number of folded layers explaining the rating of 2 points. Thus, the column harness continuously is folded with only one layer, which gives those 3 points each. The folding directions of option A-III are inversed, which gives the main harness the better folding situation (3 points). However, at some points, 15 layers of the column harness need to get folded at once then. Achieving an accurate folding with this many layers of Flex PCB is considered as almost impossible, which justifies the rating of 0 points.

Except of the indispensable gaps for the folding between the *PVG's*, the *area* of the main harness is the only bigger area without photovoltaic. This *area* is kept to a minimum by option A-II and A-III (3 points), which are only different in the order of folding. The dimensions of A-I's main harness are bound to the dimensions of the PVG's. Therefore, a bigger area is occupied by the main harness, inferentially a relatively smaller area can be used to accommodate PVG's, and hence only 2 points are given.

With the given points, option A-II scores highest with 76.58 % followed by option A-I with 64.08 %. Option A-III only scores 50.67 %. Due to the fact that option A-III can only hardly be accomplished with the current flex PCB design it will no longer be pursued.

5.2 Folding of the Column Harness (B)

5.2.1 Evaluation Criteria and Weighting (B)

Dimensioning, *integration* and *stowing* are already explained in Chapter 5.1.1.Compared to the other criteria they are of less importance with weighting factors between 4.55 and 6.36, whereas the other criteria are in the range between 8.18 and 12.73.

The space which is needed for the harness loops in stowed configuration is described by the *volume* criteria. Since all folding options are implemented by the same material (Flex PCB), the mass difference is taken into account by the *volume* criteria as well. In stowed configuration *elastic force* is generated by the harness, with the consequence that the harness pops out of the accommodation box when released. Therefore, the *elastic force* preferably shall be kept to a minimum to also reduce the necessity of deployment support structures. The loops of the stowed harness not only generate an *elastic force* and take up space but also increase the risk of breaking due to the small bending radius, considering the high loads during take-off. For this reason, the possibility of breaking (*conductibility*) of the conducting paths options shall be regarded.

During deployment, the *uniformity* and the *load on the booms* are evaluated. The *uniformity* refers to the angles between the generators and whether they increase simultaneously and synchronically. This allows conclusions about the predictability and therefore the controllability of the blanket. The *load on the booms* is primarily caused by the elastic force of the harness, which changes during deployment. For this reason, the rating of this criteria is based on the change of the force generated by the harness and its maximum values.

In deployed configuration, the *conductibility* is also regarded, due to the deformation of the harness. Besides the *PVG area* is considered, with the gap between the PVG as the relevant parameter.

Table 5.3 Evaluation criteria and weighting factors of design parameter B (folding of the column harness)

pre-launch activities			*stowed configuration*		
B 2.1	B 2.2	B 2.3	B 3.1	B 3.2	B 3.3
dimensioning	integration	stowing	volume	force	conductibility
5.00	6.67	7.22	11.11	8.89	13.89

deployment		*deployed configuration*	
B 4.1	B 4.2	B 5.1	B 5.2
uniformity	boom load	conductibility	PVG area
10.00	10.56	13.89	12.78

5.2.2 Evaluation of the Harness Folding Options (B)

In terms of *dimensioning*, the stowed and deployed state of the harness folding options is decisive. Option B-I is the only design, where mainly the stowed case needs to be regarded for *dimensioning*, since in deployed configuration it isn't deformed at all. For this reason, it gets 3 points and therefore 1 point more than the other options (2 points each). The *integration* of option B-I also gets a high rating (4 points), due to the fact, that with a flat harness in deployed configuration it can, unlike the other options with harness loops on both sides of the blanket's plane, be layed down. For *integration*, option B-II is considered worst with 2 points. In contrast to option B-III and B-IV (3 points each), the harness folding needs to be applied from both sides of the blanket, which implies a higher work effort. The rating of the *stowing* is based on the natural position of the harness. While option B-IV stays in *stowed* configuration by itself (4 points), option B-I is in its natural position when deployed (0 points). Option B-III can also be *stowed* good (3 points), because the plastic deformation defines the motion of the *stowing*. Then again option B-II can just hardly be *stowed* without any additional structures (deployment support structures), explaining the rating of 1 point.

Regarding the *volume*, the harness loops of option B-I and B-II take up the most space (2 points each). The lowest *volume* is needed by option B-III, giving it 4 points. Option B-IV is situated in-between with 3 points. By the help of the force-distance diagram (Figure 4.6) the *force* and the related pop-out effect of the harness folding options are evaluated. With no pop out at all, option B-IV gets an ideal rating of 4 points. Options B-I and B-II have the biggest pop-out and are therefore rated with 1 point each. 2 points are given to option B-III, due to its lower pop-out effect. In stowed state, the harness loops of option B-I and B-II are relatively big, by what the outer loops get pushed away by each other, giving them a lower bending radius and thus a higher risk of *breaking* the harness (2 points each for *conductibility*). The loops of option B-III and B-IV have a lower degree of influence on each other, which gives them a rating of 3 points.

The harness folding tests have shown, that the difference between the maximum and minimum angle of the generators varies from option to option (diagram, see appendix: Figure A.5 p. 65). Option B-I has the highest difference during the whole deployment, with an average of 39°, giving it only 0 points in terms of uniformity. In contrast option B-II and B-IV only differ by about 6° in average (3 points each) and option B-III by 15° (2 points). The evaluation of the boom load is also based on the harness folding tests, in fact, on the force-elongation diagram (Figure 4.7). For now, a smother decrease of the force is considered better as a sharp decrease, which makes option B-IV best with 3 points and option B-I worst with 1 point. Options B-II and B-III lie in-between and thus get 2 points each.

In deployed state, the *conductibility* of option B-I and B-II is ensured (4 points each), due to the fact, that option B-I isn't deformed at all, and the elastic deformation of B-II is controlled by the membrane foil. Option B-III is considered worst, because of the plastic deformation (2 points). Especially the repetitive deploying and stowing for the ground tests and thus the dynamic loads can cause a breakage of conducting paths. With the stuck together loop, option

B-IV only uses elastic deformation when deployed. Because the elastic deformation is not limited by a membrane foil as in option B-II, a slightly lower rating of 3 points is given. Regarding the *area*, which can be occupied by *PVG*, ergo the gaps between the PVG, options B-III and B-IV can achieve the smallest gaps and therefore have a rating of 3 points each. Because of the pure elastic deformation of option B-I, relatively huge gaps are necessary (1 point). Option B-II accomplishes smaller gaps than B-I, due to the extra length of the harness. However, option B-II still needs bigger gaps than options B-III and B-IV and therefore gets 2 points.

With the given rating, option B-IV has by far the highest score of 77.78 %. Second best is option B-III with 65.69 %. Option B-I has the lowest score of 44.86 %, whereas Option B-II is rated slightly better with 55.42 %. It is notable, that the results of the evaluation of the harness folding designs are in the same order as the natural positions of those. The closer a design options natural position is to deployed state, the higher is its score.

5.3 Deployment Support Structures (D, E)

5.3.1 Evaluation Criteria and Weighting (D, E)

The majority of evaluation criteria are already explained in the previous chapters (5.1.1, 5.2.1).

What primarily counts for the launch vehicle is the *mass* of its payload. Depending on the design option, deployment support structures also bring a not to be neglected mass with them, which needs to be part of the evaluation

The deployment support structures are primarily designed to support the deployment process. However, if somehow a deployment support structure not only *supports* the deployment but also the blanket when it's deployed, this shall also be regarded.

Table 5.4 Evaluation criteria and weighting factors of design parameter D, E (deployment support structures)

general	*pre-launch activities*			*stowed configuration*	
D, E 1.1	D, E 2.1	D, E 2.2	D, E 2.3	D, E 3.1	D, E 3.2
mass	dimensioning	integration	stowing	volume	homogeneity
9.72	5.56	7.64	7.64	12.50	14.58

deployment		*deployed*
D, E 4.1	D, E 4.2	D, E 5.1
uniformity	boom load	support
16.67	13.89	11.81

5.3.2 Evaluation of the Deployment Support Structures (D, E)

Although the deployment support structures are subdivided in first (D) and second (E) deployment direction, they are evaluated together. This can be done, because D-I and D-II are the same design options as E-I and E-II and therefore get the same rating anyway.

Compared to the other options, the guide wires (D-II, E-II) have the highest *mass* (1 point). Not only the guide wires itself, but also the necessary structures to uncoil the guide wires need to be regarded for the *mass criterion*. With most likely metal parts but in different quantities, option D-I, E-I (lamella leaves in stowage box) and E-IV (friction clips) are placed in mid-range with 3 and 2 points. The lamella leaves on the blanket (E-V) are considered to be the most lightweight support structures and therefore get a rating of 4 points.

Guide wires affect the design of the deployment units, which implies a higher work effort in terms of *dimensioning* (1 point). Compared to that, the other design options can be *dimensioned* with less work effort and therefore get 3 points each. Option E-IV and E-V are attached directly to the blanket which makes the *integration* more difficult (2 points each). Option D-II, E-II needs *integration* work to be done on the blanket and the deployment unit, by what it gets one point less (1 point). Then again, option D-I, E-I is mounted to the stowage box, making *integration* more simple, which explains the rating of 3 points. Regarding the *stowing* properties, option D-I, E-I and option D-II, E-II get 3 points and option E-IV and E-V 2 points. The reason for this is that for option E-IV and E-V each friction clip/lamella leaf needs to be set up manually and additionally, when stowed, it cannot be controlled whether all clips/ lamella leaves are in place. In comparison, option D-I, E-I and D-II, E-II need less work effort for *stowing*.

In stowed configuration, the lamella leaves (D-I, E-I and E-V) only take up a relative small space. Although the leaves have a big surface, they sit between the blanket stacks and increase the overall *volume* just insignificantly (4 points each). The *volume* of the friction clips is a little bigger and rated with 3 points. The guide wires only get a rating of 1 point, because additional structures to uncoil the wires are necessary. In terms of *homogeneity*, the guide wires are best with 4 points, for the reason that they are stowed separately and not inside the blanket stack. The only interface between the blanket and the guide wires are the eyelets. Even though the lamella leaves are slim and similar to the layers of the blanket, they most likely won't be of the same size and therefore reduce the *homogeneity* of the whole stack. Because of this, both lamella leaf options (D-I, E-I and E-V) get 2 points. Due to the shape of the friction clips, it is not recommended to compress the blanket in this area. The disruption of the homogeneous blanket by the friction clips is the reason for the 1 point rating.

During the deployment, the behavior of all options, except the guide wires, is considered to be similar. In all three cases (option D-I, E-I, option E-IV, option E-V), the blanket has to overcome a certain force, either the elastic force of the lamella leaves, or the frictional force of the friction clips, to be released and deployed. This, on one side, affects the *boom load*, due to peaks of the deployment force, and on the other side the *uniformity* of the deployment,

because an oscillation is induced. Since the friction clips and the lamella leaves on the blanket, sit on the diagonal axis and get pulled open sideways, a torque, which causes a bending of the booms, is induced when not deployed simultaneously and symmetrically (see deployment test). Therefore, in terms of boom load, option D-I, E-I gets a total of 3 points and option E-IV and E-V 2 points each. The guide wires are rated best with 4 points. The *uniformity* gets the identical rating as the *boom load.*

In contrast to the other designs, the guide wires, not only *support* the blanket during deployment, but also in deployed state. Due to the wire, which is threaded through eyelets on the blanket, a better natural oscillation and a higher stiffness can be achieved. Therefore, option D-II, E-II gets 3 points in terms of *support* in deployed state, whereas the other options get 0 points each.

With the given points, the guide wires achieve the highest rating of 68.58 %. The lamella leaves in the stowage box come next with 65.63 %. The friction clips get the worst rating with 44.97 % and the lamella leaves have a score of 56.60 %.

5.4 Total Ranking

The total ranking of the isolated evaluation can be seen in **Table 5.5**. Regarding the harness position and folding, option A-II (main harness in first deployment direction) and B-IV (bottom to bottom) have the best scoring. In contrast to the parameters A and B, the design options of the deployment support structures don't exclude each other and several options can be used at once. In this case the guide wires (D-II, E-II) have the highest ranking.

Table 5.5 Total scores of the isolated evaluation

A	Harness Position	A-II	A-I	A-III	
		76.58 %	64.08 %	50.67 %	
B	Harness Folding	B-IV	B-III	B-II	B-I
		77.78 %	65.69 %	55.42 %	44.86 %
C	Deployment Support Structures	D-II, E-II	D-I, E-I	E-V	E-IV
		68.58 %	65.63 %	56.60 %	44.97 %

6 Global Evaluation

After the design options have been evaluated within their design parameter, overall concepts shall be defined and evaluated. The determination of the weighting factors and the actual evaluation is performed with the Analytic Hierarchy Process (AHP).

The AHP is a theory and methodology for relative measurement to organize and analyze complex decisions, based on mathematical comparison [8] [9]. The Idea of the AHP is to translate the hierarchical decision making problem into a series of pairwise comparison matrices and to obtain the preference information for the attributes by the use of the eigenvector method [10].

In comparison to the utility analysis, the AHP is a much more complex and time-consuming method. A subsequent adding of alternatives (in this case design options/concepts) can be done more easily for the utility analysis as for the AHP. Additionally, the adding of alternatives to the AHP can cause rank reversals[9]. [11]

Why then use the AHP? The rank reversal is primarily not seen as a problem for the global evaluation, since only the best ranked option is decisive. Furthermore, the work effort is kept to a minimum since only one evaluation needs to be done. Then again, a pro of the AHP is, that the ranking can be checked in terms of consistency, making the results more reliable [11]. Additionally, due to the wider scale (**Table 6.1**) used for the AHP, also a more differentiated ranking can be achieved.

Table 6.1 Pairwise comparison scale of the AHP [10]

Importance	*Definition*	*Explanation*
1	equal importance	Two activities contribute equally to the objective.
3	moderate importance of one over another	Experience and judgment slightly favor one activity over another.
5	strong importance	Experience and judgment strongly favor one activity over another.
7	very strong or demonstrated importance	An activity is favored very strongly over another; its dominance demonstrated in practice.
9	extreme importance	The evidence favoring one activity over another is of the highest possible order of affirmation.
2,4,6,8	Even numbers indicate intermediate values	
Reciprocals of above	If activity *i* has one of the above numbers as-signed to it when compared with activity *j*, then j has the reciprocal value when compared with *i*.	

[9] The phenomenon of rank reversal describes the change of the original ranking, when a new alternative is added subsequently (e.g. first: A-B-C, then: D-B-A-C)

6.1 Overall Concepts

For the evaluation three concepts with a promising interaction between the individual design options are defined. Therefore, also the results of the isolated evaluation are considered. The concepts are marked in the morphological box (**Table 6.2**) and described in the following sections.

The main harness of concept 1 lies underneath the stowed package when folded (A-I). This not only gives it a better stowage volume, but also better conditions for the friction clips (E-IV). Since the folded stacks of the first folding direction directly face each other, the deployment of both sides can be supported by one friction clip for each row, and therefore, in this area, a symmetric deployment can be guaranteed. To also get a better control of the deployment in first deployment direction, lamella leaves in the stowage box shall be used (D-I). The harness folding is accomplished with a plastic deformation (B-III). However, for concept 1 it is crucial that the amount of main harness layers is kept to a minimum (C-min).

With also a plastically deformed harness (B-III), concept 2 strives for a slightly different strategy. The main harness shall be in first deployment direction (A-II), and because it then lies in a separated gap, friction clips would not assure a symmetrical deployment. Therefore, the slightly better rated lamella leaves on the blanket are used instead (E-V). In first deployment direction are also lamella leaves in the stowage box applied (D-I). However, in contrast to concept 1, the amount of main harness layers does not affect the design options (C-min – C-max).

Table 6.2 Morphological box including all design parameters, design options and the three concepts

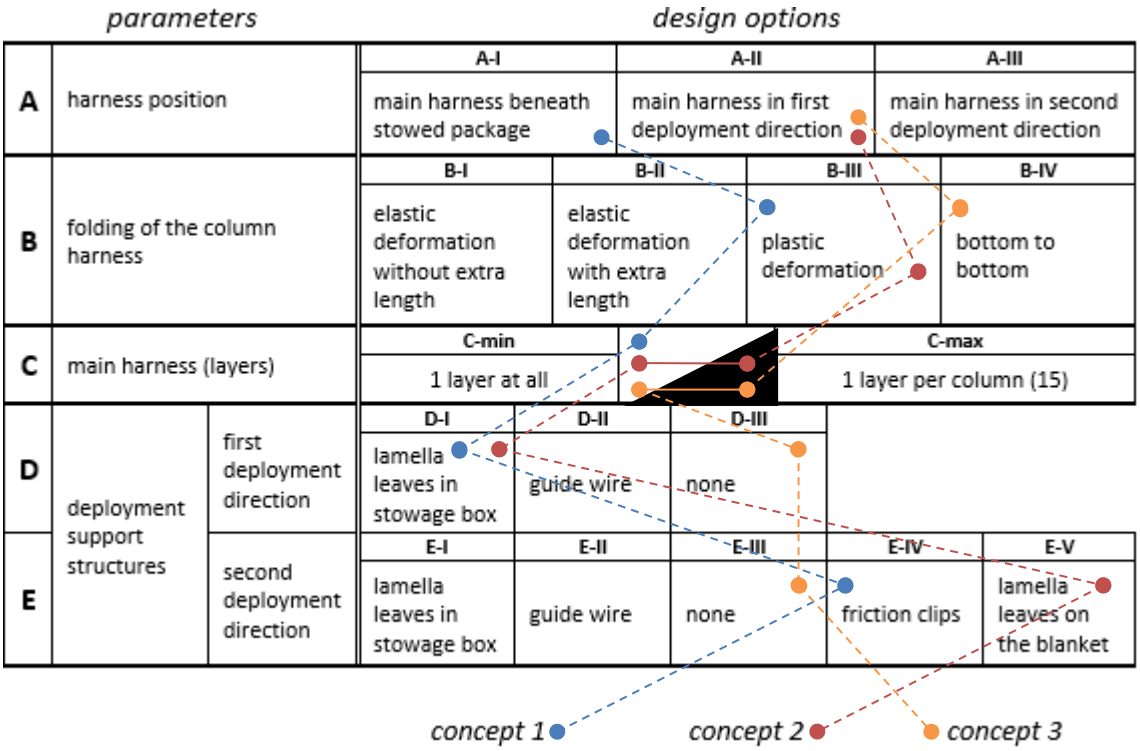

Concept 3 uses a bottom to bottom connection for the harness folding (B-IV). Due to the good deployment properties of this folding technique, no deployment support structures shall be used at all (E-III, D-III). Then again concept 3 also has the main harness in first deployment direction (A-II; C-min – C-max).

Since the guide wires (D-II, E-II) lock the blanket in place and additionally increase the overall stiffness in deployed state, they are considered beneficial for all three concepts. However, they shall not be part of the global evaluation, because when added to all three concepts, they have no influence on the results anyway.

6.2 Evaluation Criteria and Weighting

For the global evaluation, the most decisive evaluation criteria of the isolated evaluation are selected (**Table 6.3**). A detailed explanation of those can be found in the Chapters 5.1.1, 5.2.1 and 5.3.1. The mathematical approach for the weighting factors is the same as for the evaluation and therefore, shall be described in this chapter.

The pairwise comparison matrix of the weighting factors can be found in the appendix (Table A.9 p. 71). Thereby every weighting factor gets compared with every other weighting factor by dint of the AHP scale (Table 6.1). The actual weighting factors are described by the eigenvector of the matrix. To obtain the eigenvector, first, the matrix gets multiplied by itself. Then the normalized row sum represents the eigenvector. The squaring of the matrices is repeated until the difference between the current and the previous eigenvector is reduced to a minimum. For this evaluation, it is considered sufficient to square the matrix three times.

Besides the eigenvector, the consistency ration (CR) is the second important key figure of the AHP. It describes how good the rating, in terms of logic[10], is. The lower the CR Value is, the higher the consistency. An ideal consistency cannot be achieved in most cases, especially with such big matrices. Therefor CR values less than 0.10 are considered sufficient, whereas ratings with higher CR values need to be revised. A detailed explanation of the calculation of the CR can be found in literature ([12] Chapter 2.3).

Table 6.3 Evaluation criteria and weighting factors of the global evaluation (CR of matrix = 0.039)

pre-launch activities			*stowed configuration*	
GE 2.1	GE 2.2	GE 2.3	B 3.1	B 3.2
dimensioning	integration	stowing	volume	homogeneity
2.16	3.51	5.12	10.56	21.80

deployment		*deployed*
B 4.1	B 4.2	B 5.1
uniformity	boom load	PVG area
23.49	19.60	13.75

[10] E.g. if B is twice as good as A, and C twice as good as B, an ideal constancy would be gained, when C is rated four times better than A.

6.3 Evaluation of Overall Concepts

For the actual evaluation, the three concepts get compared pairwise with respect to every evaluation criterion (matrices see appendix: Table A.12 p. 74 - Table A.19 p. 76). The rating is done by comparing the individual ratings of the isolated evaluation and having also regard of the interaction between design options. For each matrix, the eigenvector gets calculated in the same way as for the weighting factors. The eigenvectors and thus the score of each concept in comparison to the other concept in each evaluation criterion, are shown in **Table 6.4**. To gain the total score, each individual score of the respective concept gets multiplied by the associated weighting factor. Those values summed up then yield the total ranking

Concept 3 has got by far the best total score with 61,58 %. Concept 1 and 2 have a similar rating of 20.36 % and 18.06 %. The excellent score of concept 1 is achieved due to the fact, that no deployment support structures are used and despite this the deployment is still considered better than the deployment of the other concepts. Therefore concept 3 has got the best rating in most of the criteria and thus hast got the best overall ranking.

Table 6.4 Global evaluation rating

	pre-launch			*stowed*
	dimensioning	integration	stowing	volume
	GE 2.1	GE 2.2	GE 2.3	GE 3.1
weighting factors	0.0216	0.0351	0.0512	0.1056
concept 1	0.101	0.088	0.078	0.691
concept 2	0.226	0.195	0.171	0.218
concept 3	0.674	0.717	0.750	0.091

stowed	*deployment*		*deployed*
homogeneity	constancy	boom load	PVG area
GE 3.2	GE 4.1	GE 4.2	GE 5.2
0.2180	0.2349	0.1960	0.1375
0.102	0.195	0.172	0.143
0.172	0.088	0.102	0.429
0.726	0.717	0.726	0.429

7 Breadboard Model (BB-2)

Due to concept 3 has by far the highest score of the global evaluation, it shall function as baseline design for the breadboard model BB-2. Within this work, the BB-2 is used to perform a first deployment test. In Addition, the BB-2 shall be used for future deployment tests.

7.1 Layout

Just like BB-1, BB-2 has got 7x7 PVG dummies on each quarter, ergo a total of 112 (**Figure 7.1**). The PVG dummies sit on the column harness, which again is attached to the main harness on the orthogonal axis. In contrast to BB-1, BB-2's column harness is as wide as the PVG dummies (100 mm). Then again, every pair of column harnesses is attached to the main harness, although the layers of the main harness only increase every second column harness. For the mechanical connection 100 mm wide strips of polyimide foil (25 µm) run perpendicular and underneath the columns. Those are also connected to the outer edge, which consists of Kapton loops with a string inside. The strings are threaded through the Kapton loops from one corner of the blanket to the next corner. For the folding of the column harness, design B-IV is used, whereas for the main harness only every second fold is done with the B-IV design and the rest initially with the B-II design (**Figure 7.3**).

The used materials are largely the same as for the BB-1. The column harness consists of a Flex PCB with a continuous copper layer of 35 µm and a 50 µm polyimide layer which is facing upwards when integrated. The main harness is a symmetric Flex PCB with 25 µm polyimide, 35 µm copper and 25 µm polyimide. Due to a change of the PVG design, the dummies are represented by only 50 µm thick Kapton patches.

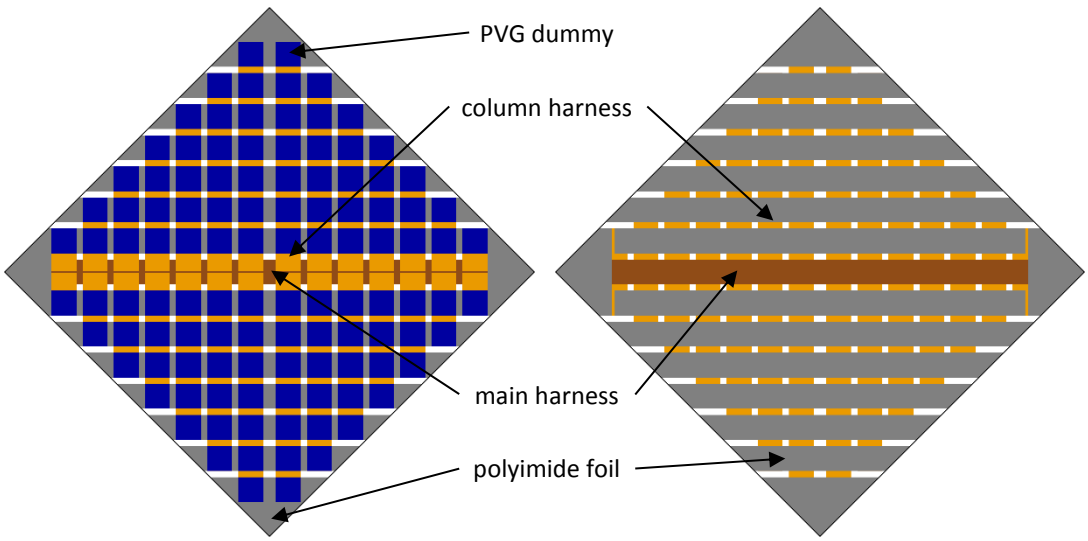

Figure 7.1 Top (left) and bottom (right) view of the breadboard-2 layout

7.2 Deployment Test

7.2.1 Setup

The deployment tests were carried out with a cross, which has got a linear guidance on the horizontal axis. Thereby, the cross is set up vertically but slightly inclined, to reduce the effect of gravity. The Blanket is mounted to the top and bottom of the cross, whereas only the second deployment direction gets deployed (**Figure 7.2**). Additionally, a force gauge is attached to the right side of the blanket.

It has become clear, that the deployment via the strings is not functioning as intended. At some points, the loose strings get stuck inside the Kapton loops and hence don't allow a sufficient deployment. Furthermore, the strings don't transmit the tensile force efficiently to the entire blanket. The triangular polyimide foil pieces at each corner of the blanket were found out to be a better force transmission point. Because of this, Kapton loops were attached to the triangles as deployment interfaces.

Figure 7.2 Deployment sequence of BB-2 in second deployment direction

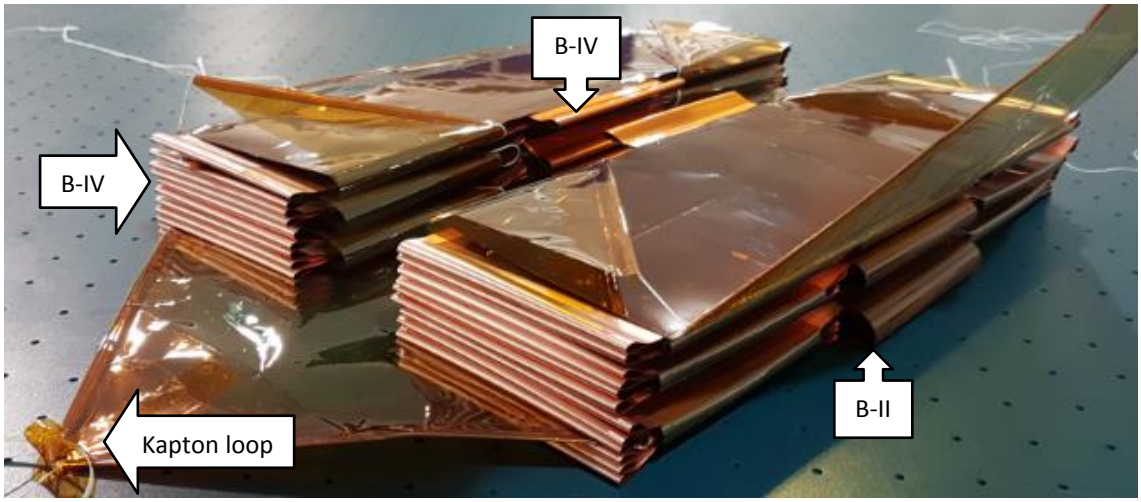

Figure 7.3 BB-2 in stowed configuration (without 90° bends in center)

7.2.2 Results

The force gauge showed a maximum force of 10.32 N, although the blanket was sufficiently deployed at about 5.5 N. The course of force during the deployment is shown in **Figure 7.4**. Until 25 s the deployment is considered predominantly uniform, whereas after 25 s the graph's course is disturbed due to the manual deployment. It can be seen, that the uniform deployment has got an exponential character (trend line: $y = 0.0397e^{0.1816x}$). This means that the force as a function of the distance is exponential too. In addition, no peak loads occur during the deployment. These are ideal conditions for a predictable and controllable deployment. However, for the actual technology demonstrator with a total of 480 PVG's and 336[11] more harness folds than the BB-2, the force in deployed state, which is generated by the harness folds, most likely needs to be decreased. The course of force can be influenced by the actual dimensions of the harness folding (B-IV). With bigger gaps between the PVG's and a longer elastically deformed harness between the PVG and the harness loop, the course of force can be overall decreased.

Comparing BB-2 with BB-1, BB-2 shows a smoother rise of force without any peaks (in second deployment direction). Additionally, no asymmetrical deployment was notices. Nevertheless, a direct comparison of the deployment and the progression of force shall be done with the results of future deployment tests with the same setup as for the BB-1 deployment test. However, it can also be said, that the self-stowing of BB-2 simplifies the handling of the blanket. It not only stays in stowed configuration by itself, but also no additional deployment support structures need to be setup.

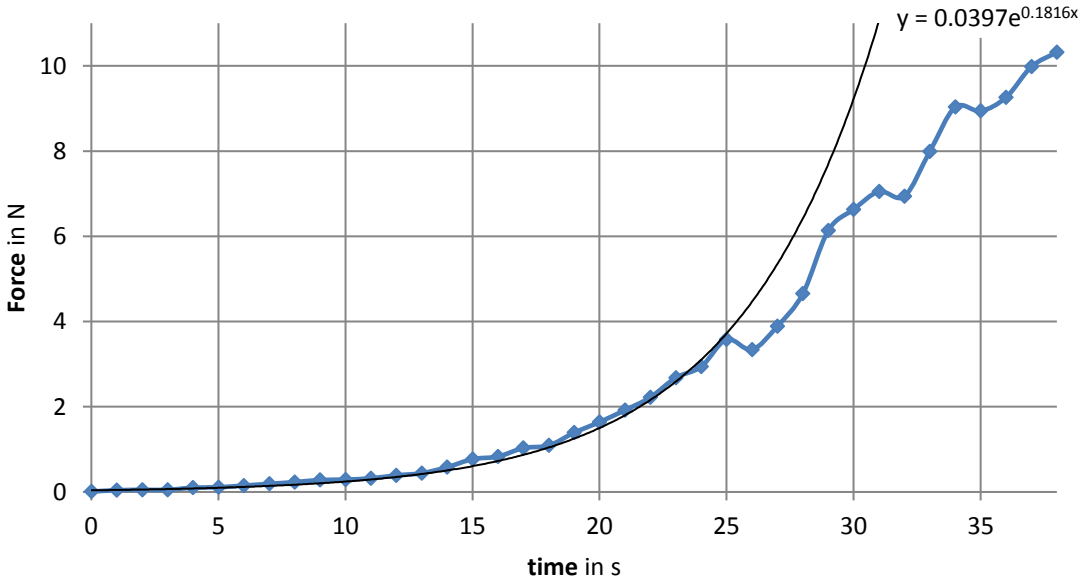

Figure 7.4 Force-time diagram of the BB-2 deployment test

[11] For the calculation of harness folds, it needs to be considered, that the first row does not get folded (A-II). Therefore, the BB-2 with a total of 112 PVG's has 84 harness folds $(112 - 4 \cdot 7 = 84)$ and the technology demonstrator 420 harness folds $(480 - 4 \cdot 15 = 420)$.

8 Conclusion

Within this bachelor thesis it was proofed, that a completely new deployment strategy, namely a strategy for which extra deployment support structures are dispensable, constitutes a superior deployment. The core of it is the design of the 180° bend of the harness, because of its relatively high elastic forces. Whereas three of the four harness folding designs cause the blanket to pop out of the stowage box (Figure 4.6 p. 28), which needs to be prevented by deployment support structures, the fourth, so-called bottom to bottom design option (B-IV) stays in stowed configuration by itself. This is because for the bottom to bottom design, the harness gets attached to itself after the 180° turn and therefore won't change this state unless it gets pulled open by external forces. However, the bottom to bottom design not only entails a better deployment but also an overall less complex design. Due to the fact, that no support structures are needed, the overall work effort decreases significantly in terms of dimensioning, integration but also stowing, since the blanket gets stowed by itself. Although for the bottom to bottom design more force is needed to deploy the blanket, no possibly even higher load peaks on the booms are triggered. Except for the guide wires, all examined deployment support structures cause peak loads on the booms, some even bending (Figure 4.3 p. 25). Then again, the course of force of the bottom to bottom design during deployment, although it is one with the highest forces, is considered better, because it doesn't increase as fast and sharp as the others (Figure 4.7 p. 29). The advantage of this lies in the fact, that with a smoother increase of force, the deployed state can be set in a wider range and on the other hand, there's a smaller risk of breaking the booms. Then again, the deployed state has not been determined yet. Considering it at 165° between the PVG's, still 99,14 % of the sunlight's energy would be received by the Generators. In a deployed state of 165°, all four harness folding options are still in the linear zone and their deployment force only varies slightly (Figure 4.8 p. 30). This means that the difference between the deployment forces is lower than initially anticipated.

After two evaluations proofed the bottom to bottom design (Isolated Evaluation p. 33) and the overall concept (Global Evaluation p. 41) including the bottom to bottom folding (concept 3) as superior, concept 3 was realized as a breadboard model. A first deployment test showed, that the deployment without deployment support structures is possible and especially easier to handle. The measured course of force of the second deployment direction has an exponential graph without any peaks, which indicates an ideal deployment in terms of predictability and controllability.

9 Outlook

Since the Breadboard (BB-2) includes the most important discoveries and innovations of this bachelor thesis, it is now indispensable to initially continue the development process by carrying out deployment tests in a more realistic scenario. Preferably the tests shall be performed in the same way as the test for the BB-1 to make both comparable to each other. This, in particular, would be beneficial, because the BB-1 represents some of the other concepts. However, some improvements should be done at the breadboard model before the tests start. Since the string loop solution doesn't work out as intended, the outer edge of the blanket shall be replaced by a continuous connection to obtain a better flux of force. Another problem which occurred, was that some harness folds (B-IV) were released. This can be fixed by wrapping a 5 mm Kapton tape around the harness layers at the bottom of the loops.

During the harness folding tests no significant bending was transmitted from the harness folds to the PVG's/ the PVG dummies. However, the thickness of the PVG's has decreased and therefore the bending of the PVG's needs to be examined again with the slimmer PVG's (dummies). Since the BB-2 is equipped with already the slim PVG dummies, this also can be done within the deployment tests.

The current bottom to bottom design consists of an elastically deformed harness loop, which is exposed to a primarily static load. In order to achieve better conditions in terms of volume and mass, the minimization of the bending radius to a plastic deformation can be examined. Additionally, the dimensioning parameters of the bottom to bottom design option can be used to lower the course of force during deployment and therefore the force, which is needed in deployed state.

The increase of stiffness and the locking effect of guide wires are considered as an advantageous quality for the whole blanket. However, guide wires also entail an influence on the deployment units. Therefore, it should be investigated how big the influences are and whether they can be accepted.

Another open topic is the design of the main harness and most of all the connection between the main harness and the column harness. An answer to this question is essential for the further development process.

Bibliography

[1] C. H. M. Jenkins and P. Zarchan, Gossamer Spacecraft: Membrane and Inflatable Structures Technology for Space Applications, Virginia: American institute of Aeronautics and Astronautics, Inc., 2001.

[2] T. Sproewitz, P. Seefeldt, J.-T. Grundmann, P. Spietz, N. Toth, M. Hillebrandt, M. Straubel and M. Zander, "Design of the Gossamer-1 Deployment Demonstrator," Bremen, Braunschweig.

[3] E. Howell, "Space," 7 Feb. 2018. [Online]. Available: https://www.space.com/16748-international-space-station.html. [Accessed 24 April 2018].

[4] M. Garcia, "NASA," 4 Aug. 2017. [Online]. Available: https://www.nasa.gov/mission_pages/station/structure/elements/solar_arrays-about.html. [Accessed 24 April 2018].

[5] California Institute of Technology, "Mars InSight Mission," [Online]. Available: jpl.nasa.gov. [Accessed 2 Mai 2018].

[6] Orbital ATK, "orbitalatk," 2018. [Online]. Available: https://www.orbitalatk.com/space-systems/space-components/solar-arrays/default.aspx. [Accessed 2 Mai 2018].

[7] O. Mori, H. Sawada, R. Funase, M. Morimoto, T. Endo, T. Yamamoto, Y. Tsuda, Y. Kawakatsu and J. Kawaguchi, "First Solar Power Sail Demonstration by IKAROS," JAXA Space Exploration Center, Sagamihara, Japan, 2010.

[8] M. Brunelli, Introduction to the Analytic Hierarchy Process, Springer International Publishing, 2015.

[9] Institute of Space Systems, "GoSolAr - Concurrent Engineering Study Report," Bremen, 2016.

[10] X. Sun, "Multiple Criteria Decision Analysis Techniques in Aircraft Design and Evaluation Processes," Technischen Universit□at Hamburg-Harburg, Xinxiang, China, 2012.

[11] R. Riedl, "Analytischer Hierarchieprozess vs. Nutzwertanalyse," in *Wirtschaftsinformatik als Schlüssel zum Unternehmenserfolg*, Wiesbaden, Deutscher Universitats-Verlag, GWV Fachverlage GmbH, 2006, p. 289.

[12] M. P.-R. Enrique Mu, *Practical Decision Making - An Introduction to the Analytic Hierarchy Process (AHP) Using Super Decisions v2,* Pittsburgh, PA: Springer International Publishing AG Switzerland, 2017.

[13] Technische Universität München, *Analytischer Hierarchieprozess (AHP) - Methodik der multikriteriellen Bewertung,* 2015.

List of Figures

List of Tables

A Appendix

A.1 BB-1 Deployment Tests

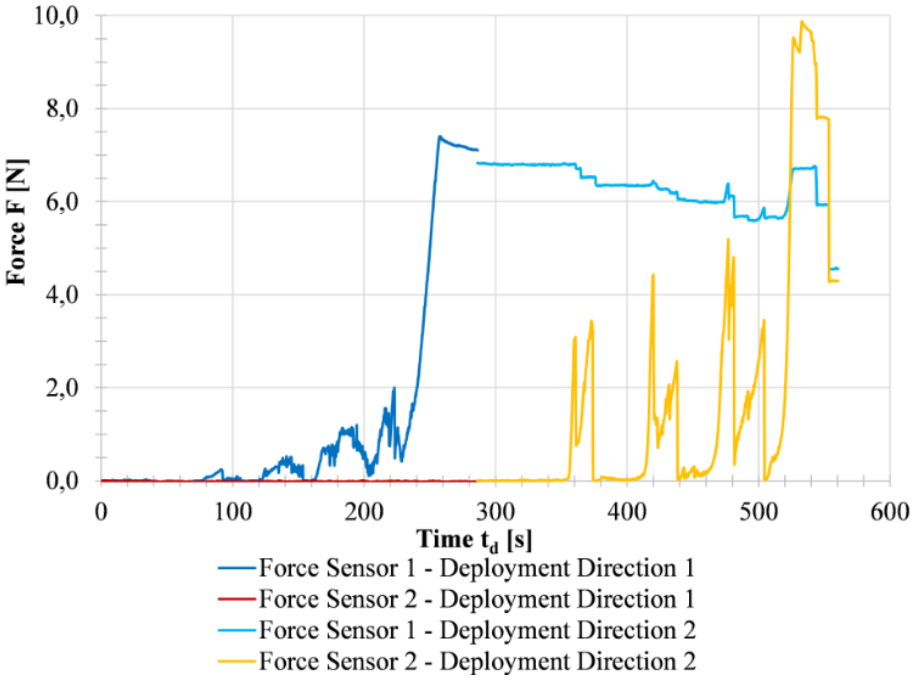

Figure A.1 Force-time diagram run #1; blanket orientation: booms underneath; blanket supported w. foam block; PVG pointing upwards

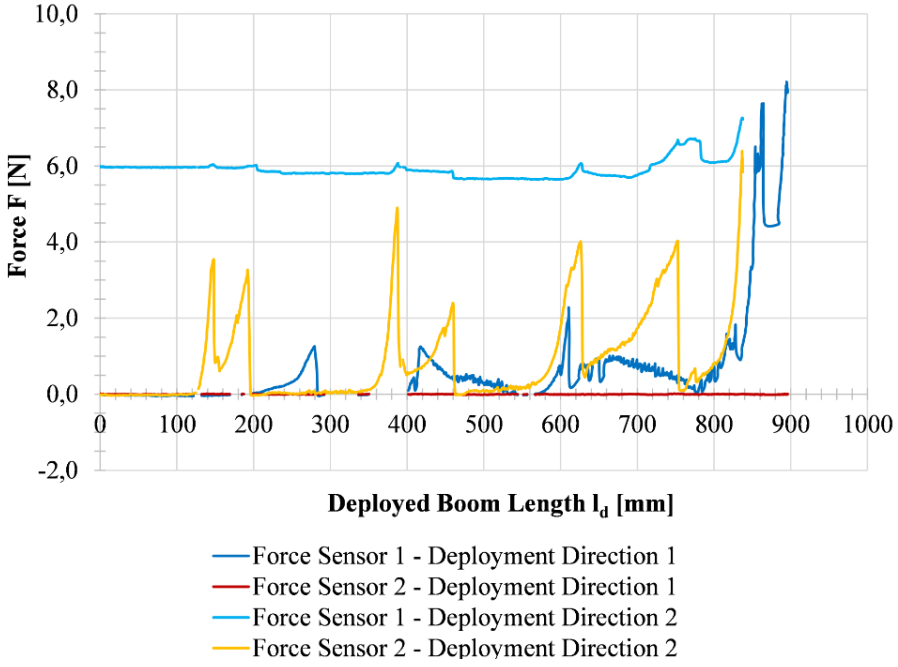

Figure A.2 Force-distance diagram: run #1; blanket orientation: booms underneath; blanket supported w. foam block; PVG pointing upwards

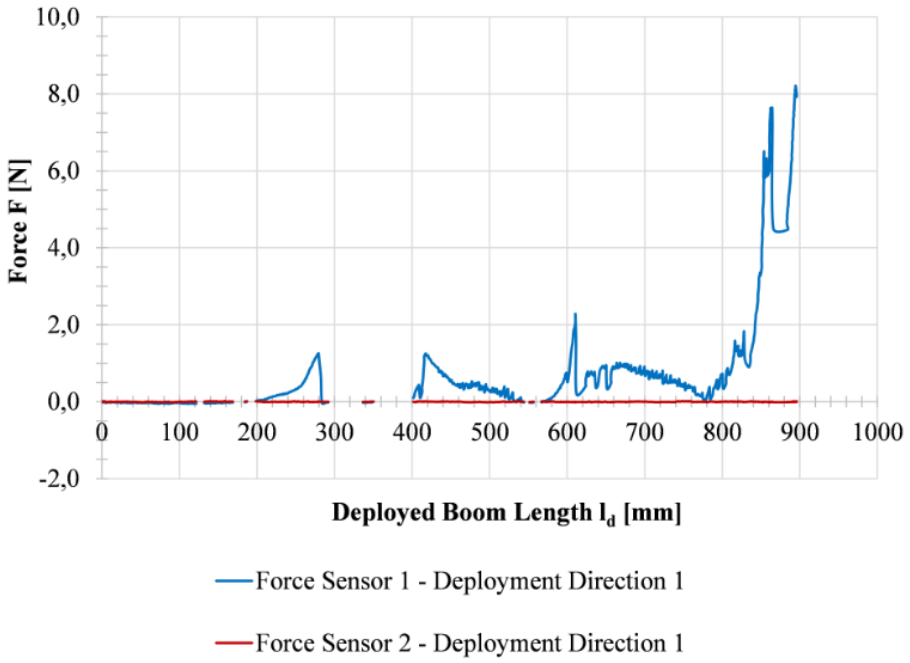

Figure A.3 Force-distance diagram: run #2; blanket orientation: booms underneath; blanket supported w. foam block; PVG pointing upwards; deployment direction 1

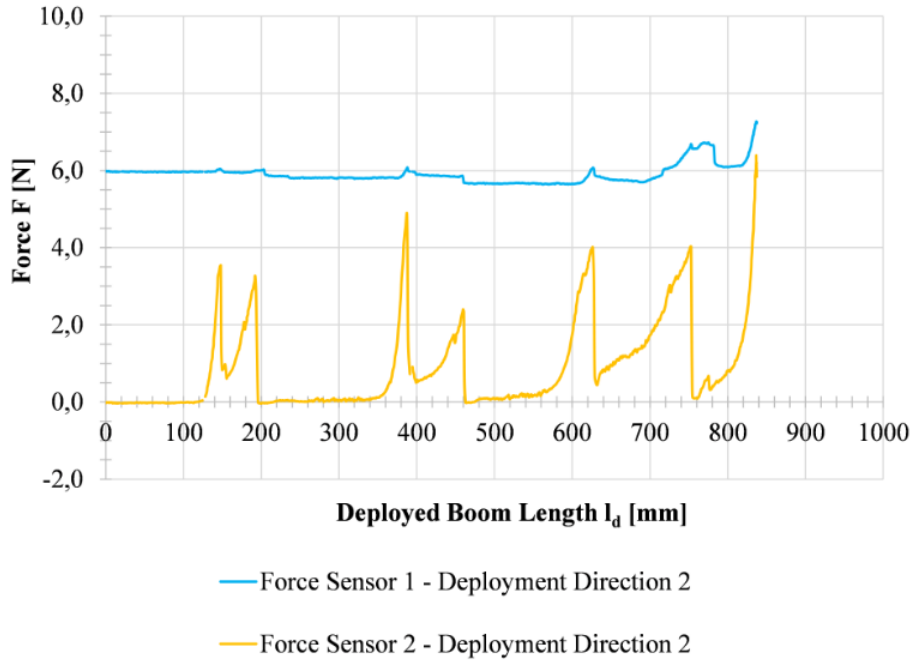

Figure A.4 Force-distance diagram: run #2; blanket orientation: booms underneath; blanket supported w. foam block; PVG pointing upwards; deployment direction 2

Table A.1 Harness folding test measurement data: B-I

B-I: Elastic Deformation without Extra Length											Date:		07.06.2018	
											Time:		14:00	
Nb.	***absolute Distance*** *in cm*	***relative Distance*** *in cm*	***Force*** *in N*			***Angle*** *in °*								
			X	***Y***	***Z***	***1-2***	***2-3***	***3-4***	***4-5***	***1***	***2***	***3***	***4***	***5***
1	62.1	0.5	-0.297	0.041	7.143									
2	62.6	1	-0.25	0.346	3.794									
3	63.1	1.5	-0.172	0.152	2.936									
4	63.6	2	-0.031	0.069	2.15									
5	64.6	3	-0.14	-0.014	1.251									
6	65.6	4	-0.14	0.014	0.496									
7	66.6	5	-0.094	0.069	0.103									
8	68.6	7	-0.109	0.055	0.083									
9	70.6	9	-0.109	0.028	0.083									
10	75.6	14	-0.109	0.014	0.072									
11	80.6	19	-0.109	0	0.052									
12	85.6	24	-0.109	0	0.021									
13	90.6	29	-0.125	0	0.021									
14	95.6	34	-0.125	0.014	0.021									
15	100.6	39	-0.14	0.014	0.01	89.7	60.2	32.9	17.8	39.6	50.7	69.1	78	84.2
16	105.6	44	-0.156	0.014	0.01	94.4	70.5	47.2	37.8	38.7	46.9	62.6	70.2	72
17	110.6	49	-0.156	0.028	-0.021	107.7	86.1	63.2	46.4	32.6	39.7	54.2	62.6	71
18	115.6	54	-0.172	0.041	-0.062	124	108.7	86.7	57.6	25.9	30.1	41.2	52.1	70.3
19	120.6	59	-0.187	0.055	-0.083	128.8	114.2	97.2	78.1	23.9	27.3	38.5	44.3	57.6
20	125.6	64	-0.203	0.041	-0.093	139.8	130.1	116.8	97.3	19.4	20.8	29.1	34.1	48.6
21	130.6	69	-0.219	0.083	-0.3	153.7	146.6	135	121.1	14.6	11.7	21.7	23.3	35.6
22	133.6	72	-0.219	0.111	-0.548	162.3	158.3	149.1	137.3	10.4	7.3	14.4	16.5	26.2
23	135.6	74	-0.25	0.097	-0.961	171	171.3	165	154.6	6.7	2.3	6.4	8.6	16.8
24	136.6	75	-0.265	0.097	-1.592	175.2	176.3	175.3	171.6	3.8	1	2.7	2	6.4
25	137	75.4	-0.312	0.097	-10	177.6	178.2	178	177.6	1.8	0.6	1.2	0.8	1.6

Table A.2 Harness folding test measurement data: B-II

B-II: Elastic Deformation with Extra Length													Date:	07.06.2018
													Time:	16:10
Nb.	**absolute Distance** in cm	**relative Distance** in cm	**Force** in N			**Angle** in °								
			X	**Y**	**Z**	**1-2**	**2-3**	**3-4**	**4-5**	**1**	**2**	**3**	**4**	**5**
1	62.1	0.5	-0.14	0.927	9.499									
2	62.6	1	-0.265	0.844	3.38									
3	63.1	1.5	-0.094	0.609	2.584									
4	63.6	2	-0.109	0.387	2.057									
5	64.6	3	-0.187	0.221	1.178									
6	65.6	4	-0.172	0.152	0.517									
7	66.6	5	-0.109	0.138	0.124									
8	68.6	7	-0.078	0.124	0.083									
9	70.6	9	-0.078	0.083	0.083									
10	75.6	14	-0.109	0.055	0.083									
11	80.6	19	-0.109	0.055	0.072									
12	85.6	24	-0.109	0.041	0.052									
13	90.6	29	-0.109	0.041	0.031									
14	95.6	34	-0.125	0.028	0.01									
15	100.6	39	-0.14	0.041	0.021	58.6	48.6	45	46.5	58.4	63	68.4	66.6	66.9
16	105.6	44	-0.14	0.041	0	68.2	59	55.6	57.8	54.1	57.7	63.3	61.1	61.1
17	110.6	49	-0.156	0.028	-0.01	76.1	71.1	70	72.7	50.8	53.1	55.8	54.2	53.1
18	115.6	54	-0.172	0.028	-0.041	89.5	84.8	82.5	84.6	44.8	45.7	49.5	48	47.4
19	120.6	59	-0.187	0.028	-0.083	103.9	101	98.2	98.6	38.1	38	41	40.8	40.6
20	125.6	64	-0.203	0.028	-0.207	122.8	116.5	113.8	114.8	27.3	29.9	33.6	32.6	32.6
21	128.6	67	-0.219	0.041	-0.444	139.1	131.5	126	124.1	18.8	22.1	26.4	27.6	28.3
22	130.6	69	-0.219	0.041	-0.693	151.1	143.9	137.4	134.1	12.9	16	20.1	22.5	23.4
23	131.6	70	-0.234	0.041	-0.765	145.5	146	147.5	149.2	17.2	17.3	16.7	15.8	15
24	132.6	71	-0.219	0.069	-1.271	159.6	155.8	152.8	151.7	9.4	11	13.2	14	14.3
25	133.6	72	-0.234	0.083	-2.212	168.5	166.9	164.8	163.4	5.5	6	7.1	8.1	8.5
26	134.1	72.5	-0.297	0.097	-4.714	172.2	171.8	171	171.1	3.9	3.9	4.3	4.7	4.2
27	134.5	72.9	-0.328	0.124	-10	175.9	175.8	175.4	176.1	2.1	2	2.2	2.4	1.5

Table A.3 Harness folding test measurement data: B-III

B-III: Plastic Deformation													Date:	07.06.2018
													Time:	17:00
Nb.	**absolute Distance** in cm	**relative Distance** in cm	**Force** in N			**Angle** in °								
			X	**Y**	**Z**	**1-2**	**2-3**	**3-4**	**4-5**	**1**	**2**	**3**	**4**	**5**
1	62.1	0.5	-0.437	0.498	9.272									
2	62.6	1	-0.297	0.277	4.155									
3	63.1	1.5	-0.234	0.29	2.367									
4	64.1	2.5	-0.187	0.18	0.403									
5	65.1	3.5	-0.14	0.18	0.124									
6	70.1	8.5	-0.109	0.083	0.103									
7	75.1	13.5	-0.14	0.069	0.093									
8	80.1	18.5	-0.125	0.041	0.072									
9	85.1	23.5	-0.125	0.041	0.062									
10	90.1	28.5	-0.125	0.041	0.021									
11	95.1	33.5	-0.109	0.028	0.01									
12	100.1	38.5	-0.109	0.028	0	81.1	66.6	55.1	48.2	45.7	53.2	60.2	64.7	67.1
13	105.1	43.5	-0.125	0.028	-0.01	90.2	78.9	69	62.1	42	47.8	53.3	57.7	60.2
14	110.1	48.5	-0.14	0.028	-0.031	99.4	91.6	84.5	78	38.4	42.2	46.2	49.3	52.7
15	115.1	53.5	-0.14	0.028	-0.052	108.2	103.3	98.9	95.5	34.7	37.1	39.6	41.5	43
16	120.1	58.5	-0.172	0.028	-0.134	124	118.7	112	107.9	27	29	32.3	35.7	36.4
17	123.1	61.5	-0.203	0.055	-0.217	134.8	129.4	122.5	118.5	21.4	23.8	26.8	30.7	30.8
18	126.1	64.5	-0.203	0.083	-0.475	149.5	142.8	135.7	131.5	13.8	16.7	20.5	23.8	24.7
19	128.1	66.5	-0.219	0.069	-0.775	159.6	154.3	148.9	144.7	8.8	11.6	14.1	17	18.3
20	129.1	67.5	-0.219	0.069	-1.085	165.4	161.9	158.1	154.4	6.4	8.2	9.9	12	13.6
21	130.1	68.5	-0.234	0.069	-2.005	171.8	170.7	168.6	167.6	4.1	4.1	5.2	6.2	6.2
22	130.6	69	-0.343	0.083	-5.716	176.7	175.6	174.7	175.2	1.5	1.8	2.6	2.7	2.1
23	130.8	69.2	-0.359	0.097	-10	176.5	176.5	176.4	176.8	1.7	1.8	1.7	1.9	1.3

Table A.4 Harness folding test measurement data: B-IV

B-IV: Bottom to Bottom													Date:	07.06.2018
													Time:	15:25
Nb.	***absolute Distance*** *in cm*	***relative Distance*** *in cm*	***Force*** *in N*			***Angle*** *in °*								
			X	***Y***	***Z***	***1-2***	***2-3***	***3-4***	***4-5***	***1***	***2***	***3***	***4***	***5***
1	62.1	0.5	-0.484	0.871	0.951									
2	62.6	1	-0.281	0.719	0.062									
3	63.6	2	0.031	0.29	0.021									
4	65.6	4	-0.109	0.138	0.031									
5	70.6	9	-0.078	0.055	-0.01									
6	75.6	14	-0.156	0.069	0									
7	80.6	19	-0.125	0.041	-0.041									
8	85.6	24	-0.14	0.041	-0.052									
9	90.6	29	-0.14	0.041	-0.062									
10	95.6	34	-0.14	0.028	-0.062									
11	100.6	39	-0.156	0.028	-0.072	81.2	78.1	75.2	73.6	48.4	50.4	51.5	53.3	53.1
12	105.6	44	-0.156	0.028	-0.103	95	91.1	88.2	88.1	41.7	43.3	45.6	46.2	45.7
13	110.6	49	-0.156	0.028	-0.134	107.3	105.6	103.9	103.4	36.4	36.3	38.1	38	38.6
14	115.6	54	-0.156	0.041	-0.196	120.7	119.9	120.3	121.6	29.5	29.8	30.3	29.4	29
15	120.6	59	-0.187	0.083	-0.538	146.3	141.8	135.6	131.4	16.3	17.4	20.8	23.6	25
16	122.6	61	-0.172	0.111	-0.879	156.5	152	145.8	140.4	11.1	12.4	15.6	18.6	21
17	123.6	62	-0.187	0.111	-1.127	162	157.6	151.1	146	8.5	9.5	12.9	16	18
18	124.6	63	-0.187	0.124	-1.292	165.4	162.4	157.1	152.9	7.2	7.4	10.2	12.7	14.4
19	125.6	64	-0.187	0.124	-1.644	169	167.2	164	161.4	5.7	5.3	7.5	8.5	10.1
20	126.6	65	-0.203	0.111	-2.222	172.2	171.2	169.7	169.9	4.3	3.5	5.3	5	5.1
21	127.1	65.5	-0.219	0.111	-2.739	173.3	172.7	171.7	172.4	3.8	2.9	4.4	3.9	3.7
22	127.6	66	-0.234	0.111	-3.618	175.1	174.2	173	173.5	2.9	2	3.8	3.2	3.3
23	128.1	66.5	-0.25	0.124	-4.693	177.3	176.2	174.7	175.2	1.8	0.9	2.9	2.4	2.4
24	128.6	67	-0.281	0.138	-6.367	177.7	178	176.6	175.6	2.1	0.2	1.8	1.6	2.8
25	129.1	67.5	-0.328	0.111	-10	177.9	178.1	178.4	178.1	1.2	0.9	1	0.6	1.3

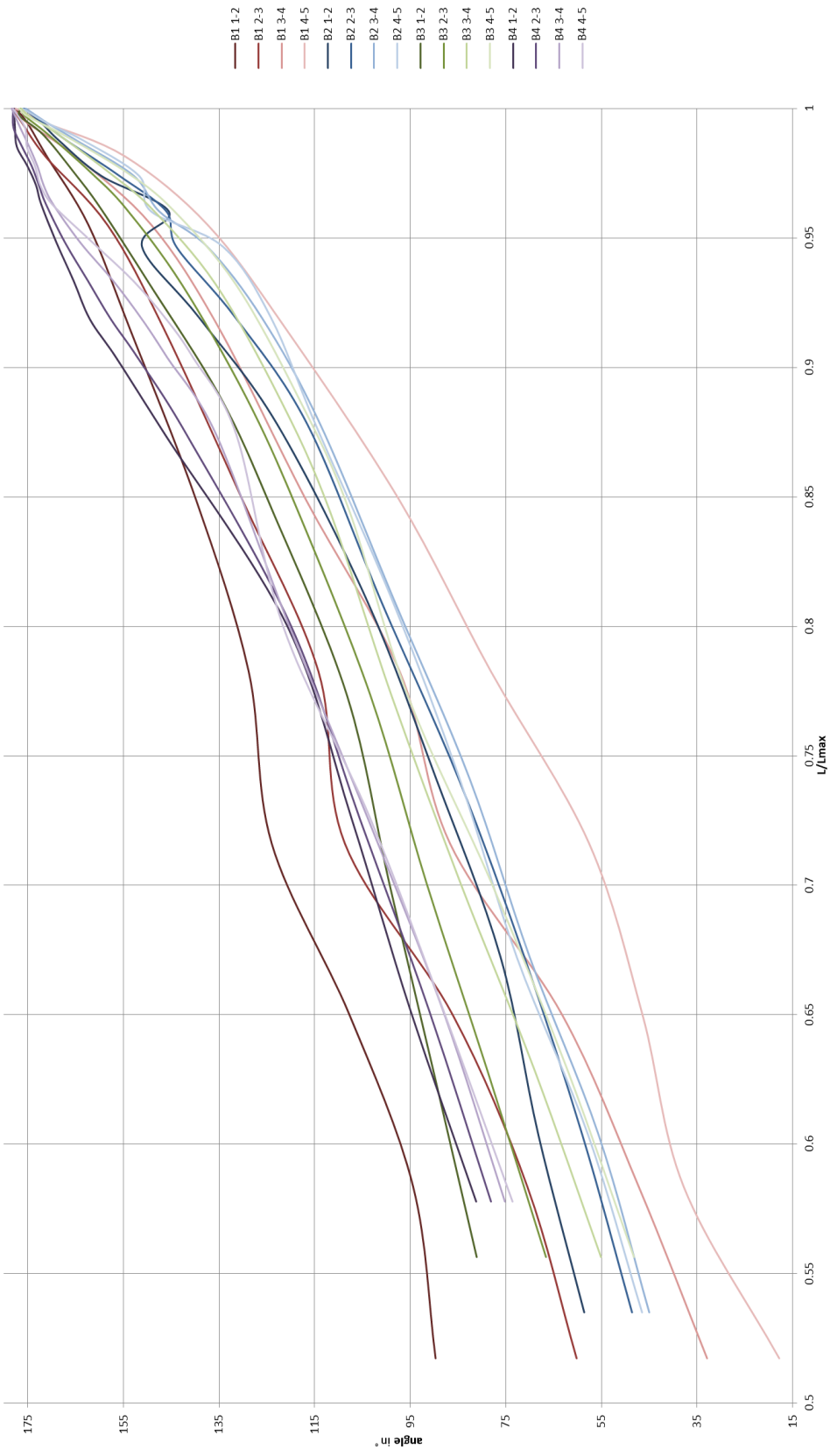

Figure A.5 Angle-elongation diagram showing all 4 angles of all 4 design options, each option in one colour range

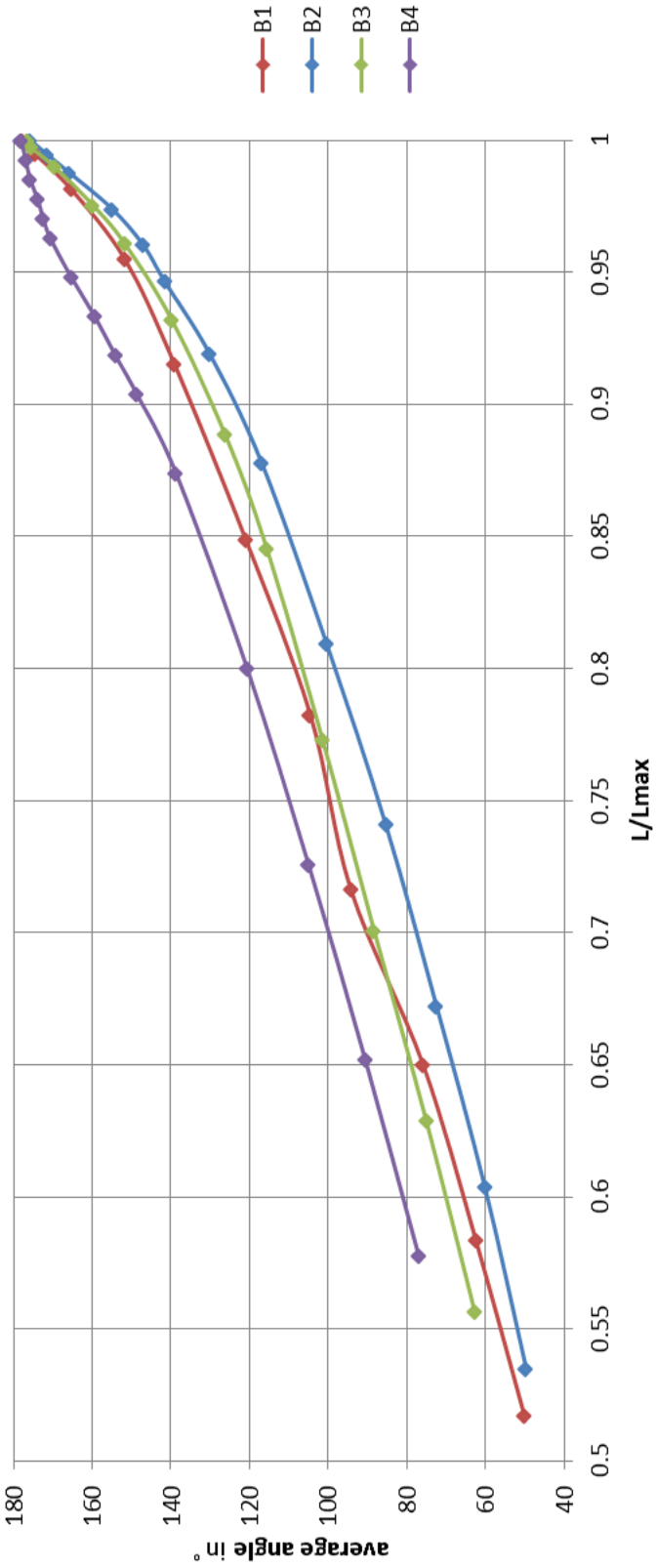

Figure A.6 Angle-elongation diagram with the average angle

Table A.5 Pairwise comparison matrix of the weighting factors of the harness position (A)

Harness Position

A

main criteria

comparing...

	with...	*pre-launch activities*			*stowed configuration*		*deployed*
		A 2.1	A 2.2	A 2.3	A 3.1	A 3.2	A 5.1
		dimensioning	integration	stowing	volume	homogeinity, accuracy of stacks	PVG area
A 2.1	dimensioning	0	3	3	3	3	3
A 2.2	integration	1	0	2	3	3	3
A 2.3	stowing	1	2	0	3	2	3
A 3.1	volume	1	1	1	0	2	2
A 3.2	homogeinity	1	1	2	2	0	1
A 5.1	PVG area	1	1	1	2	3	0
score		5	8	9	13	13	12
rank		6	5	4	1	1	3
weighting factors		0.0833	0.1333	0.1500	0.2167	0.2167	0.2000
		8.33	13.33	15.00	21.67	21.67	20.00

overall: 60

check sum

1

100 %

%

subcriteria

	A 3.2.1	A 3.2.2
	main harness	column harness
weighting factors	0.4	0.6

Table A.6 Evaluation table of harness position (A)

Harness Position

A	evaluation criteria		weighting factor	option A-I		option A-II		option A-III	
				rating	weighted rating	rating	weighted rating	rating	weighted rating
main criteria	A 2.1	dimensioning	0.0833	2	0.167	4	0.333	1	0.083
	A 2.2	integration	0.1333	2	0.267	4	0.533	1	0.133
	A 2.3	stowing	0.1500	2	0.300	4	0.600	2	0.300
	A 3.1	volume	0.2167	4	0.867	2	0.433	3	0.650
	A 3.2	homogeneity	0.2167	2.6	0.563	2.6	0.563	1.2	0.260
	A 5.1	PVG area	0.2000	2	0.400	3	0.600	3	0.600
		check sum:	1						
subcriteria	A 3.2.1	main harness	0.4	2	0.8	2	0.8	3	1.2
	A 3.2.2	column harness	0.6	3	1.8	3	1.8	0	0
grand total				0.641		0.766		0.507	
				64.08		76.58		50.67	%

Table A.7 Pairwise comparison matrix of the weighting factors of the harness folding (B)

Harness Folding

B

main criteria

comparing...

		pre-launch activities			*stowed configuration*			*deployment*			
		B 2.1	B 2.2	B 2.3	B 3.1	B 3.2	B 3.3	B 4.1	B 4.2	B 5.3	B 5.4
	with...	dimensioning	integration	stowing	volume	force	conductibility	uniformity	boom load	conductibility	PVG area
B 2.1	dimensioning	0	3	3	3	3	3	3	3	3	3
B 2.2	integration	1	0	2	3	3	3	3	3	3	3
B 2.3	stowing	1	2	0	3	2	3	3	3	3	3
B 3.1	volume	1	1	1	0	1	3	2	2	3	2
B 3.2	force	1	1	2	3	0	3	2	2	3	3
B 3.3	conductibility	1	1	1	1	1	0	1	1	2	2
B 4.1	uniformity	1	1	1	2	2	3	0	2	3	3
B 4.2	boom load	1	1	1	2	2	3	2	0	3	2
B 5.3	conductibility	1	1	1	1	1	2	1	1	0	2
B 5.4	PVG area	1	1	1	2	1	2	1	2	2	0

score	9	12	13	20	16	25	18	19	25	23	***overall:***	180
rank	10	9	8	4	7	1	6	5	1	3		

												check sum
weighting factors	0.0500	0.0667	0.0722	0.1111	0.0889	0.1389	0.1000	0.1056	0.1389	0.1278		1
	5.00	6.67	7.22	11.11	8.89	13.89	10.00	10.56	13.89	12.78	%	100 %

Table A.8 Evaluation table of harness folding (B)

Harness Folding

B	evaluation criteria		weighting factor	option B-I		option B-II		option B-III		option B-IV	
				rating	weighted rating	rating	weighted rating	rating	weighted rating	rating	weighted rating
main criteria	B 2.1	dimensioning	0.0500	3	0.150	2	0.100	2	0.100	2	0.100
	B 2.2	integration	0.0667	4	0.267	2	0.133	3	0.200	3	0.200
	B 2.3	stowing	0.0722	0	0.000	1	0.072	3	0.217	4	0.289
	B 3.1	volume	0.1111	2	0.222	2	0.222	4	0.444	3	0.333
	B 3.2	force	0.0889	1	0.089	1	0.089	2	0.178	4	0.356
	B 3.3	conductibility	0.1389	2	0.278	2	0.278	3	0.417	3	0.417
	B 4.1	uniformity	0.1000	0	0.000	3	0.300	2	0.200	3	0.300
	B 4.2	boom load	0.1056	1	0.106	2	0.211	2	0.211	3	0.317
	B 5.3	conductibility	0.1389	4	0.556	4	0.556	2	0.278	3	0.417
	B 5.4	PVG area	0.1278	1	0.128	2	0.256	3	0.383	3	0.383
		check sum:	1								
subcriteria											
	grand total			0.449		0.554		0.657		0.778	
				44.86		55.42		65.69		77.78	%

Table A.9 Pairwise comparison matrix of the weighting factors of the deployment support structures (D, E)

Deployment Support Structures

D, E

main criteria

comparing...

		general	*pre-launch activities*			*stowed configuration*		*deployment*		*deployed*
		D,E 1.1	D,E 2.1	D,E 2.2	D,E 2.3	D,E 3.1	D,E 3.2	D,E 4.1	D,E 4.2	D,E 5.1
	with...	mass	dimensioning	integration	stowing	volume	homogeneity	uniformity	boom load	support
D,E 1.1	mass	0	1	1	1	3	3	3	3	3
D,E 2.1	dimensioning	3	0	3	3	3	3	3	3	3
D,E 2.2	integration	3	1	0	2	3	3	3	3	3
D,E 2.3	stowing	3	1	2	0	3	3	3	3	3
D,E 3.1	volume	1	1	1	1	0	3	3	2	2
D,E 3.2	homogeneity	1	1	1	1	1	0	3	2	1
D,E 4.1	uniformity	1	1	1	1	1	1	0	1	1
D,E 4.2	boom load	1	1	1	1	2	2	3	0	1
D,E 5.1	support	1	1	1	1	2	3	3	3	0

score	14	8	11	11	18	21	24	20	17	***overall:***	144
rank	6	9	7	7	4	2	1	3	5		
											check sum
weighting factor	0.0972	0.0556	0.0764	0.0764	0.1250	0.1458	0.1667	0.1389	0.1181		1
	9.72	5.56	7.64	7.64	12.50	14.58	16.67	13.89	11.81	%	100

Table A.10 Evaluation table of deployment support structures (D, E)

Deployment Support Structures

D, E	evaluation criteria		weighting factor	option D-I, E-I		option D-II, E-II		option E-IV		option E-V	
				rating	weighted rating	rating	weighted rating	rating	weighted rating	rating	weighted rating
main criteria	D,E 1.1	mass	0.0972	3	0.292	1	0.097	2	0.194	4	0.389
	D,E 2.1	dimensioning	0.0556	3	0.167	1	0.056	3	0.167	3	0.167
	D,E 2.2	integration	0.0764	3	0.229	1	0.076	2	0.153	2	0.153
	D,E 2.3	stowing	0.0764	3	0.229	3	0.229	2	0.153	2	0.153
	D,E 3.1	volume	0.1250	4	0.500	1	0.125	3	0.375	4	0.500
	D,E 3.2	homogeneity	0.1458	2	0.292	4	0.583	1	0.146	2	0.292
	D,E 4.1	uniformity	0.1667	3	0.500	4	0.667	2	0.333	2	0.333
	D,E 4.2	boom load	0.1389	3	0.417	4	0.556	2	0.278	2	0.278
	D,E 5.1	support	0.1181	0	0.000	3	0.354	0	0.000	0	0.000
		check sum:	1								
subcriteria											
	grand total			0.656		0.686		0.450		0.566	
				65.63		68.58		44.97		56.60	%

Table A.11 Pairwise comparison matrix of the weighting factors of the global evaluation

		pre-launch			*stowed configuration*		*deployment*		*deployed*		
		dimensioning	integration	stowing	volume	homogeneity	constancy	boom load	PVG area	**weighting**	
comparing...		GE 2.1	GE 2.2	GE 2.3	GE 3.1	GE 3.2	GE 4.1	GE 4.2	GE 5.2	**factors:**	*ranking*
GE 2.1	dimensioning	1	1/3	1/4	1/6	1/6	1/7	1/7	1/7	0.0216	8
GE 2.2	integration	3	1	1/2	1/4	1/5	1/6	1/6	1/5	0.0351	7
GE 2.3	stowing	4	2	1	1/3	1/4	1/5	1/5	1/3	0.0512	6
GE 3.1	volume	6	4	3	1	1/3	1/2	1/2	1/2	0.1056	5
GE 3.2	homogeneity	6	5	4	3	1	1/2	2	2	0.2180	2
GE 4.1	constancy	7	6	5	2	2	1	1	2	0.2349	1
GE 4.2	boom load	7	6	5	2	1/2	1	1	2	0.1960	3
GE 5.2	PVG area	7	5	3	2	1/2	1/2	1/2	1	0.1375	4

Table A.12 Pairwise comparison matrix of dimensioning (GE 2.1) with CR = 0.074

pre-launch	GE 2.1
dimensioning	

		with …	
comparing …	concept 1	concept 2	concept 3
concept 1	1	1/3	1/5
concept 2	3	1	1/4
concept 3	5	4	1

Table A.13 Pairwise comparison matrix of integration (GE 2.2) with CR = 0.081

pre-launch	GE 2.2
integration	

		with …	
comparing …	concept 1	concept 2	concept 3
concept 1	1	1/3	1/6
concept 2	3	1	1/5
concept 3	6	5	1

Table A.14 Pairwise comparison matrix of stowing (GE 2.2) with CR = 0.086

pre-launch	GE 2.3
stowing	

		with …	
comparing …	concept 1	concept 2	concept 3
concept 1	1	1/3	1/7
concept 2	3	1	1/6
concept 3	7	6	1

Table A.15 Pairwise comparison matrix of volume (GE 3.1) with CR = 0.046

stowed	GE 3.1
volume	

		with …	
comparing …	concept 1	concept 2	concept 3
concept 1	1	4	6
concept 2	1/4	1	3
concept 3	1/6	1/3	1

Table A.16 Pairwise comparison matrix of homogeneity (GE 3.2) with CR = 0.025

stowed	GE 3.2
homogeneity	

		with …	
comparing …	concept 1	concept 2	concept 3
concept 1	1	1/2	1/6
concept 2	2	1	1/5
concept 3	6	5	1

Table A.17 Pairwise comparison matrix of uniformity (GE 4.1) with CR = 0.081

deployment	GE 4.1
uniformity	

		with …	
comparing …	concept 1	concept 2	concept 3
concept 1	1	3	1/5
concept 2	1/3	1	1/6
concept 3	5	6	1

Table A.18 Pairwise comparison matrix of boom load (GE 4.2) with CR = 0.025

deployment	GE 4.2
boom load	

		with …	
comparing …	concept 1	concept 2	concept 3
concept 1	1	2	1/5
concept 2	1/2	1	1/6
concept 3	5	6	1

Table A.19 Pairwise comparison matrix of PVG area (GE 5.1) with CR = 0.00

deployed	GE 5.1
PVG area	

		with …	
comparing …	concept 1	concept 2	concept 3
concept 1	1	1/3	1/3
concept 2	3	1	1
concept 3	3	1	1